

Volatile Organic Compound Detection Using Insect Odorant-Receptor Functionalised Field-Effect Transistors

by

Eddyn Oswald Perkins Treacher

A thesis submitted in fulfilment of the
requirements of the degree of
Doctor of Philosophy in Physics
School of Physical and Chemical Sciences
Te Herenga Waka - Victoria University of Wellington

May 2024



Table of contents

Acknowledgements	1
1. Non-Covalent Functionalisation of Carbon Nanotube and Graphene Films	3
1.1. Introduction	3
1.2. Non-Covalent Bonding and π -Stacking	4
1.3. Attachment of 1-Pyrenebutanoic Acid N-Hydroxysuccinimide Ester	4
1.3.1. Comparing Attachment Methods	4
1.3.2. Examining 1-Pyrenebutanoic Acid N-Hydroxysuccinimide Ester Purity	8
1.3.3. Electrical Characterisation	10
1.4. Attachment of 1-Pyrenebutyric Acid	14
1.4.1. Comparing Attachment Methods	14
1.4.2. Raman Spectroscopy	14
1.4.3. Electrical Characterisation	16
1.5. Attachment of PEGlyated Pyrene-Based Linkers	18
1.5.1. Pyrene-NTA, Pyrene-Biotin and PEGylation	18
1.6. Identifying Functionalisation Obstacles using Fluorescence Microscopy	19
1.6.1. General Overview	19
1.6.2. Photoresist Contamination	20
1.6.3. Hydrophobicity of Carbon Nanotubes and Graphene	22
1.6.4. Substrate Interaction with Linker Molecules	25
1.6.5. Coffee-Ring Effect	25
1.7. Conclusion	26
Appendices	29
A. Vapour System Hardware	29
B. Python Code for Data Analysis	31
B.1. Code Repository	31
B.2. Atomic Force Microscope Histogram Analysis	31
B.3. Raman Spectroscopy Analysis	31
B.4. Field-Effect Transistor Analysis	31

Acknowledgements

69450

Rifat, Alex - vapour sensor
Erica Cassie - FET sensing setup
Rob Keyzers and Jennie Ramirez-Garcia - NMR spectra
Patricia Hunt - Computational chemistry

1. Non-Covalent Functionalisation of Carbon Nanotube and Graphene Films

1.1. Introduction

In previous chapters, I have discussed methods of fabricating carbon nanotube and graphene devices and then shown that they are sensitive to environmental changes in a saline solution. However, for specific sensing, the devices require (bio)chemical functionalisation. Instead of responding to stimuli themselves, the sensing signal is picked up by attached receptors. The devices then act as passive transducers for the received signal. Receptors previously used with carbon nanotube and graphene devices include aptamers [1]–[6] and a range of proteins [7]–[10], including animal odorant receptors [11]–[16]. A common approach to attaching receptors to the transducer involves the use of a linker molecule to tether the receptor to the transducer. Verifying that this linker molecule is bridging between the transducer and the receptor element is important for a complete understanding of the behaviour of these sensors. This verification involves providing evidence for effective attachment of linker molecule to the transducing device channel, then showing successful tethering of odorant receptors and other biomolecules to the attached linker molecule.

This chapter therefore takes some time exploring the following selection of available linker molecules for specific biosensing: 1-Pyrenebutanoic Acid N-Hydroxysuccinimide Ester (PBASE), 1-Pyrenebutyric Acid (PBA), Pyrene-PEG-NTA (PPN) and Pyrene-PEG-Biotin (PPB). The mechanisms underlying functionalisation with each linker are described. A literature review and analysis techniques including Raman spectroscopy, fluorescence microscopy and electrical characterisation are used to understand the impact of various experimental parameters on the functionalisation process. Electrical characterisation of linker attachment to the transducer was also performed to act as a comparison tool when performing functionalisation with insect odorant receptors. Numerous obstacles to successful functionalisation are identified and discussed, including PBASE hydrolysis, linker coverage, non-specific attachment, photoresist contamination, channel hydrophobicity and the coffee-ring effect. Approaches to overcome these obstacles were identified, tested and the results characterised. This process provided assurance that successful attachment of linker molecule to the carbon nanotube network or graphene channel could be achieved.

1.2. Non-Covalent Bonding and π -Stacking

Linker molecules may be attached via covalent or non-covalent bonding to carbon nanomaterials, such as carbon nanotubes and graphene. Covalent bonding is stronger than non-covalent bonding, and therefore gives a more permanent attachment between linker molecules and the transducer. Unlike covalent attachment, non-covalent attachment preserves the polycyclic sp^2 bonding of carbon atoms in graphene and carbon nanotubes and therefore the electrical properties of the channel [1], [3], [5], [10], [17]–[19]. For example, one group found covalent bonding of diazonium linker caused a $\sim 50\%$ drop in graphene channel mobility [7]. In comparison, only a $\sim 5\%$ drop in mobility was seen for attachment of a mixture of linkers containing pyrene to a graphene channel via non-covalent π stacking [20]. π -stacking or $\pi - \pi$ interaction describes a type of non-covalent bonding which occurs due to dispersion forces between unsaturated polycyclic molecules¹ [22]. A wide range of linker molecules with aromatic moieties, such as pyrene, have been used for modification of polycyclic carbon nanotubes and graphene via π -stacking [5], [22]–[24]. Figure 1.1 demonstrates the relationship between a pyrene-based linker molecule to the transducer and receptor elements. Pyrene-based π -stacking underlies all the functionalisation processes used in this thesis.

1.3. Attachment of 1-Pyrenebutanoic Acid N-Hydroxysuccinimide Ester

1.3.1. Comparing Attachment Methods

1-pyrenebutanoic acid N-hydroxysuccinimide ester (also known commercially and in the literature as 1-pyrenebutyric acid N-hydroxysuccinimide ester and 1-pyrenebutanoic acid succinimidyl ester, alongside acronyms PBASE, PBSE, PyBASE, PASE, PYSE, PSE, Pyr-NHS and PANHS) is a aromatic molecule commonly used for tethering biomolecules to the carbon rings of graphene and carbon nanotubes. Using computational modelling, two locally stable molecular conformations were found to exist, a straight (Figure 1.2a) and bent (Figure 1.2b) structure. The conformation in Figure 1.2a has a Hartree-Fock energy of -3427728.67 kJ/mol, while the conformation in Figure 1.2b has a Hartree-Fock energy of -3427729.66 kJ/mol. The difference between computed Hartree-Fock energies is 1.0 kJ/mol, small enough that the existence of both molecular conformations is physically feasible. Similar straight and bent structures have previously been modelled for PBASE attached to graphene [27].

¹It has been argued that this label is unhelpfully specific and a misrepresentation of what can be simply classed as a type of Van Der Waals bonding [21], [22]. However, as the use of the term is widespread in the literature, it is also used here for the sake of clarity.

1.3. Attachment of 1-Pyrenebutanoic Acid N-Hydroxysuccinimide Ester

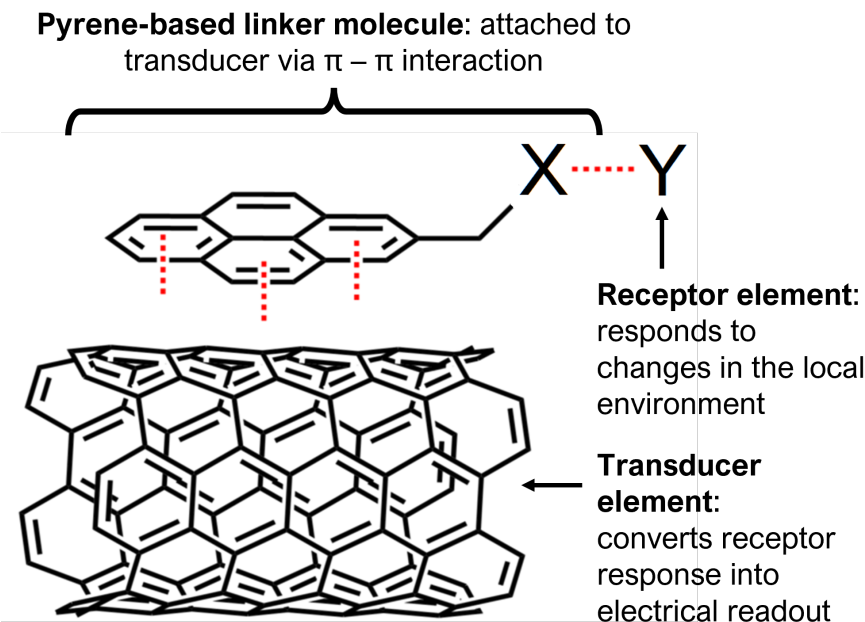


Figure 1.1.: Attachment of pyrene-based linker molecule pyrene-X and receptor Y to a carbon nanotube, representing the transducer element of a field-effect transistor. Source: Adapted from [25].

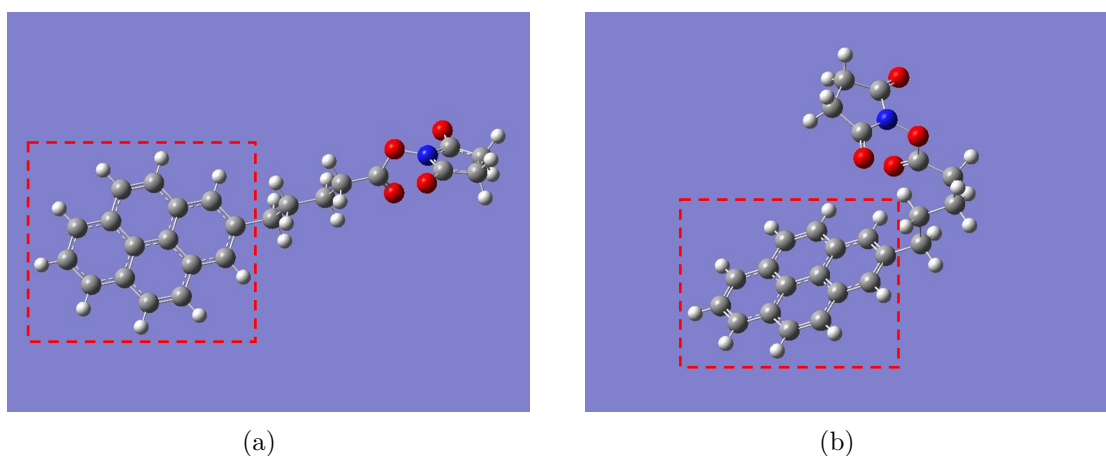


Figure 1.2.: Two conformations of PBASE molecule with geometry optimised via *ab initio* calculations performed with Gaussian 16 software [26]. White balls correspond to hydrogen, grey to carbon, red to oxygen and blue to nitrogen. The pyrene moiety is highlighted in the image with a red dashed outline.

1. Non-Covalent Functionalisation of Carbon Nanotube and Graphene Films

Table 1.1.: Comparison of PBASE functionalisation processes used for immobilisation of proteins and aptamers onto carbon nanotubes and graphene. Experimentally optimised variables are marked with a star (*). Blank entries indicate there was no mention of the parameter in a particular paper.

Solvent	Channel	Conc. (mM)	Incubation type	Time (hr)	Rinse steps	References
DMF	CNT	5	Immersed	1	PBS	Maehashi, 2007. [28]
		6	Immersed	1	DMF, PBS	García-Aljaro, 2010. [29]
		6	Immersed	1	DMF	Chen, 2001. [30]
		6	Immersed	1	DMF	Cella, 2010. [31]
		6	Immersed	1	DMF	Das, 2011. [32]
		6	-	2	DMF	Besteman, 2003. [33]
	Graphene	-	-	2	DMF	Tsang, 2019. [34]
		-	-	20	-	Wiedman, 2017. [35]
		0.2	Immersed	20	DMF, IPA, DI water	Gao, 2018. [36]
		1	Dropcast	6	DMF, IPA, DI water	Nekrasov, 2021. [4]
		5	Immersed	1	DMF, DI water	Hwang, 2016. [37]
		5*	Immersed	3*	DMF	Hao, 2020. [38]
		5	Immersed	4*	DMF, DI water	Mishyn, 2022. [5]
		6	Dropcast	2	DMF, DI water	Nur Nasufiya, 2020. [39]
		10	Dropcast	2	DMF, DI water	Campos, 2019. [40]
	Graphene	10	Immersed	2	DMF, PBS	Kuscu, 2020. [41]
		10	Immersed	1	DMF	Xu, 2017. [42]
		10	Immersed	12	DMF, EtOH, DI water	Khan, 2020. [43]
		50	Immersed	4*	MeOH	Wang, 2020. [10]
		1	Immersed	1	DI water	Ono, 2020. [44]
Methanol	CNT	1	Immersed	1	MeOH, DI water	Zheng, 2016. [45]
		1	Immersed	2	MeOH	Kim, 2009. [46]
DMSO	Graphene	100	Dropcast	1	DI water	Yoo, 2022. [16]
		5	Immersed	2	-	Sethi, 2020. [47]
		5	Immersed	1	MeOH, PBS	Ohno, 2010. [48]
	CNT	10	-	1	DI water	Lopez, 2015. [49]
		10	Immersed	1	PBS	Strack, 2013. [50]

1.3. Attachment of 1-Pyrenebutanoic Acid N-Hydroxysuccinimide Ester

The pyrene moiety, highlighted with a red dashed outline in Figure 1.2a-b, non-covalently bonds to the carbon rings of the carbon nanotube and graphene surface. The N-hydroxysuccinimide (NHS) ester group, seen on the right-hand side of Figure 1.2, is highly reactive with amine groups. It can undergo a nucleophilic substitution reaction with primary amines attached to proteins or aptamers, tethering these biomolecules via an amide or imide bond [3], [5], [23], [30], [51].

The non-covalent functionalisation of proteins onto a single-walled carbon nanotube using PBASE was first reported by Chen *et al.* in 2001 [30]. Two successful methods for protein functionalisation and immobilisation were reported, with the only differences being the solvent used to dissolve the PBASE powder (DMF, methanol) and the final concentration of the resulting solutions (6 mM, 1 mM respectively). PBASE powder appears to dissolve poorly in methanol at higher concentrations, which might explain the use of different concentrations of PBASE in each solvent. An extensive comparison of methods used in the literature for PBASE functionalisation of carbon nanotube and graphene devices with aptamers and proteins is given in Table 1.1. Several listed works directly cite Chen *et al.* when discussing functionalisation with PBASE [31], [33], [40], [45], [48]. The other works listed do not explicitly reference Chen *et al.* in their methodology; however, the frequency of methods detailing the use of 6 mM PBASE in dimethylformamide (DMF) and 1 mM PBASE in methanol indicate that other groups often loosely follow the original process used by Chen *et al..*

However, it is also apparent from Table 1.1 that there is a large degree of variation in the methods used for PBASE functionalisation. Various electrical characterisation, microscopy and spectroscopy techniques have been used to demonstrate successful functionalisation. Until recently, there has been little justification provided for the selection of variables used in the functionalisation procedure (e.g. length of time submerged in solvent containing PBASE), despite the wide-ranging use of this process in the literature [10], [52], [53]. Furthermore, a detailed investigation of PBASE functionalisation process variables has only been undertaken for graphene-based devices [5], [10], [38], [53]. This is surprising, given that multiple sources indicate a close relationship between the sensitivity of functionalised devices and the density of surface functionalisation with PBASE [51], [54], [55].

Zhen *et al.* [53], Wang *et al.* [10] and Mishyn *et al.* [5] have all claimed that carefully tuning the surface concentration of PBASE is required to avoid multilayer coverage of the graphene surface, as this negatively impacts sensing. Mishyn *et al.* [5] used cyclic voltammetry to demonstrate that less receptor attachment to the graphene surface occurs when multiple layers of PBASE are present. However, none of these groups have presented analyte sensing results from their functionalised graphene devices. In contrast, Hao *et al.* [38] found that maximising the PBASE surface coverage of a channel resulted in more sensitive aptameric sensing, thereby reaching the opposite conclusion. The inconsistency in these recent findings mean more work is needed to understand the PBASE functionalisation process to achieve optimal biosensor sensitivity. It may also

1. Non-Covalent Functionalisation of Carbon Nanotube and Graphene Films

be the case that a specific functionalisation process is required for optimal sensitivity with the use of a specific type of receptor.

Once fastened to a bioreceptor via an amide or imide bond, the attachment to the linker molecule is not easily broken. However, prior to use in functionalisation processes, the NHS ester may react with any water present. This ester hydrolysis converts PBASE to its corresponding carboxylic acid, 1-pyrenebutanoic acid (PBA), leaving it unavailable to react further with amine groups [5], [51], [56]. If the amine group functionalisation is performed within a ~ 1 hour period, with a high concentration of bioreceptor used at close to neutral pH, competing hydrolysis should not have a significantly adverse impact on the functionalisation process [51]. However, if PBASE is exposed to water during storage over a significant length of time, the presence of 1-Ethyl-3-(3-dimethylaminopropyl)carbodiimide (EDC) can be used to restore the NHS ester and enable the substitution reaction to take place (see discussion of PBA/EDC in Section 1.4).

1.3.2. Examining 1-Pyrenebutanoic Acid N-Hydroxysuccinimide Ester Purity

I purchased PBASE from two suppliers, Sigma-Aldrich and Setareh Biotech. Sigma listed DMF and methanol as suitable solvents for dissolving PBASE, alongside chloroform and dimethyl sulfoxide (DMSO). Setareh Biotech indicated methanol can be used for dissolving PBASE. The two suppliers had conflicting information for suitable storage of PBASE, where Sigma recommended room temperature storage, while Setareh Biotech recommended storage of -5 to -30°C alongside protection from light and moisture. I used nuclear magnetic resonance (NMR) spectroscopy to verify the purity of PBASE from various suppliers. As water can react with PBASE to form unwanted byproducts, it appears that protection from moisture is particularly important. A particular emphasis was placed on detecting water presence in the received samples, considering the long travel time of the PBASE with uncertain storage conditions.

Figure 1.3 compares the shapes of hydrogen NMR spectra of PBASE from each supplier when dissolved in deuterated DMSO, alongside a blank deuterated DMSO spectrum. Both PBASE samples possessed characteristic chemical shift features between 2.1 – 2.2 ppm, 2.8 – 2.9 ppm, and 3.4 – 3.5 ppm. These chemical shifts roughly correspond to those seen in previous NMR spectra for PBASE [57]. The feature at 2.50 ppm represents the deuterated DMSO solvent, while the single peak between 3.3 – 3.4 ppm represents the water present in the sample. By comparing the area of these peaks, a rough estimate of the amount of water originally present in the PBASE sample can be obtained. The H₂O:DMSO ratio is 1:7 in the blank spectrum, but $\sim 1:3$ in the provided samples, possibly indicating the introduction of water to the PBASE during production or storage. However, DMSO is strongly hygroscopic and slight differences in DMSO storage time, as well as differences in humidity during sample preparation, may have had a significant impact on this result [58]. Other impurities are also seen

1.3. Attachment of 1-Pyrenebutanoic Acid N-Hydroxysuccinimide Ester

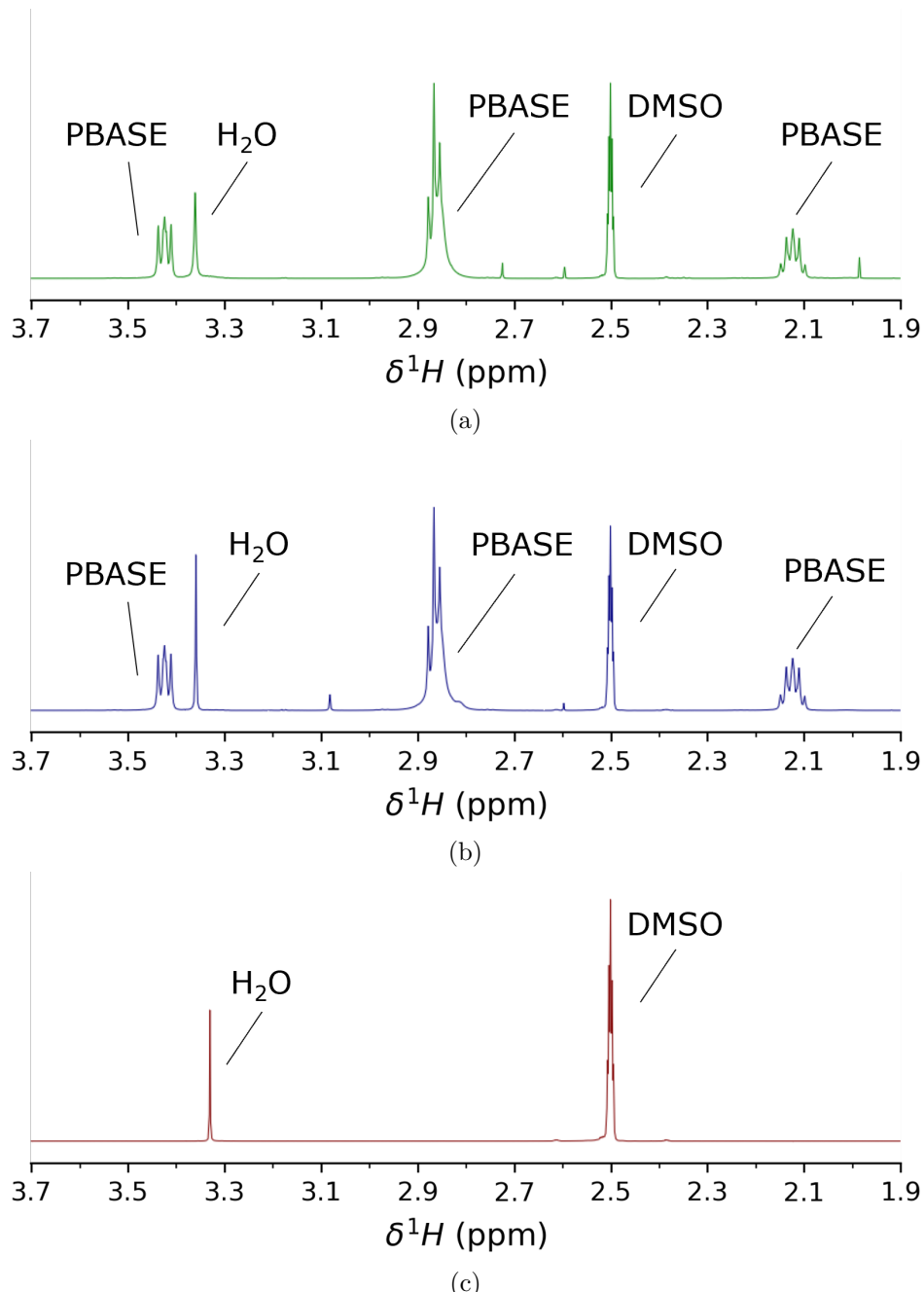


Figure 1.3.: ^1H Nuclear Magnetic Resonance (NMR) spectra, performed with DMSO- d_6 used as the NMR solvent. (a) and (b) show NMR spectrum for commercially purchased PBASE, from Sigma-Aldrich and Setareh Biotech respectively, while (c) shows the blank spectrum taken with only DMSO- d_6 present. Spectra were taken by Jennie Ramirez-Garcia, School of Chemical and Physical Sciences, Te Herenga Waka - Victoria University of Wellington. Unlabelled peaks correspond to sample impurities.

1. Non-Covalent Functionalisation of Carbon Nanotube and Graphene Films

on both PBASE spectra, though their small size indicates they make up only a small percentage of each sample. Strack *et al.* [50] recommend leaving frozen PBASE at room temperature for 15 minutes before exposing it to air to prevent condensation near the PBASE, as this can cause unnecessary H₂O contamination.

1.3.3. Electrical Characterisation

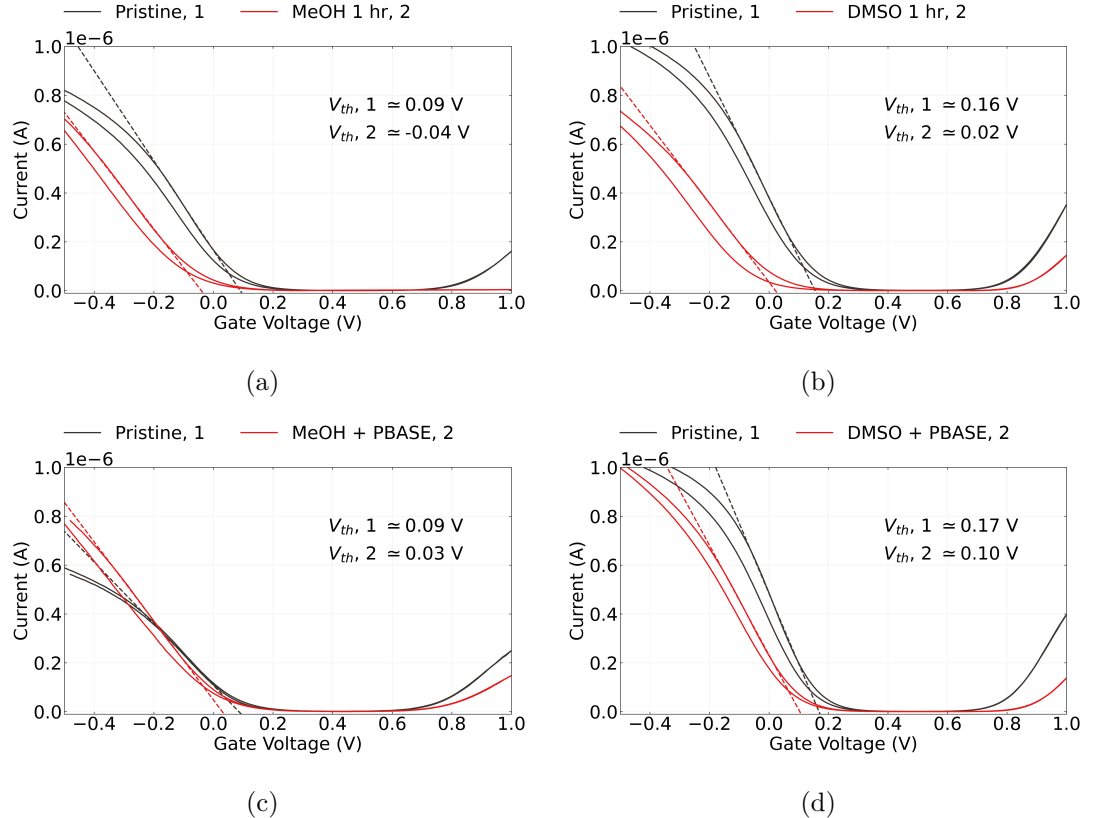


Figure 1.4.: The electrical transfer characteristics of carbon nanotube transistors ($V_{ds} = 100$ mV) before and after being submerged in methanol (a) or dimethyl sulfoxide (b) for one hour and subsequently rinsed with deionised water. The change in characteristics of similar transistor channels after being submerged in these same solvents containing 1 mM PBASE for one hour and then rinsed are shown in (c) and (d) respectively. Average threshold voltages for each transfer characteristic curve are also shown (taking the average of forward and reverse sweep values).

The electrical characteristics of the carbon nanotube or graphene transistor are often used to verify successful functionalisation and make a statement about the effect of

1.3. Attachment of 1-Pyrenebutanoic Acid N-Hydroxysuccinimide Ester

chemical modification on the channel. However, this verification usually does not account for the effect of the solvent on the transistor channel. Figure 1.4a and Figure 1.4b show that by exposing a steam-deposited carbon nanotube network channel to solvents commonly used in PBASE functionalisation processes (Table 1.1), such as methanol (MeOH) or dimethyl sulfoxide (DMSO), a significant negative shift in channel threshold voltage occurs even after thorough rinsing with deionised water. It appears that the carbon nanotubes have adsorbed solvent which persists even after thoroughly rinsing the device. From the shape of the change in the transfer curve, it seems the residual polar solvent molecules capacitively gate the channel [59], [60]. Besteman *et al.* reported observing a similar effect from prolonged exposure of a single carbon nanotube to dimethylformamide (DMF) [33]. Atomic force microscopy also indicates that solvent lingers after device cleaning. Figure 1.5 shows that after 1 hour exposure to DMSO, the feature height of the network is significantly increased.

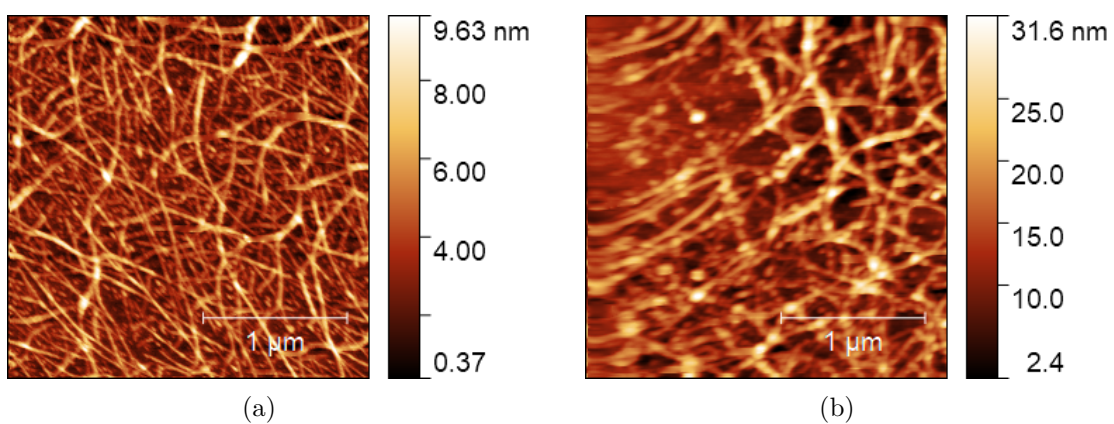


Figure 1.5.: 2.5 μm x 2.5 μm atomic force microscope images of a surfactant-deposited carbon nanotube film before (a) and after (b) 1 hour submersed in dimethyl sulfoxide (DMSO). Image blurring in (b) appears to be due to the presence of adsorped DMSO.

Capacitive gating results from dense coverage of adsorped molecules on the carbon nanotube surface which have a low permittivity relative to the surrounding electrolyte [60]. The relative permittivity of MeOH and DMSO are ~ 33 [61] and ~ 47 [62] respectively, which are both much lower than the relative permittivity of phosphate buffer saline, ~ 80 [3]. From Figure 1.4a and Figure 1.4b, the threshold shift values found resulting from exposure to each solvent, taking the average of forward and reverse sweep values from a single device, were $\Delta V = -0.15 \pm 0.02$ V and $\Delta V = -0.15 \pm 0.01$ V for MeOH and DMSO respectively. The average threshold shift value for a second device exposed to MeOH was $\Delta V = -0.16 \pm 0.02$ V, indicating that this threshold shift result is reproducible.

Using the same characterisation process as in this work, Murugathas *et al.* [13] showed that the attachment of PBASE to a solvent-deposited carbon nanotube network had little effect on channel threshold voltage, implying the presence of PBASE had not signifi-

1. Non-Covalent Functionalisation of Carbon Nanotube and Graphene Films

cantly influenced channel gating. Here, an average threshold voltage shift of -0.06 ± 0.04 V is seen after PBASE functionalisation in MeOH and -0.06 ± 0.01 V after PBASE functionalisation in DMSO. These threshold voltage shifts are small compared to solvent only. It is possible that the attachment of PBASE prevents solvent adsorption, and has a small negative gating effect on the channel. Alternatively, while the solvent negatively gates the channel, resulting in a threshold shift of -0.15 V, the PBASE may be counteracting this by positively gating the channel, resulting in a threshold shift of +0.09 V. Murugathas *et al.* also observed a slight increase in channel conductance after PBASE functionalisation [13]. Figure 1.4 also shows a slight increase in channel conductance post-functionalisation in both Figure 1.4c and Figure 1.4d relative to the solvent-only case in Figure 1.4a and Figure 1.4b. This result implies that the presence of PBASE molecules increases channel mobility and therefore conductance [60].

The absorption of organic solvent by the carbon nanotube network has unknown but potentially negative implications for biosensor functionalisation. Use of organic solvents in functionalisation can also attack the encapsulation layer of devices, promoting gate current leakage. In light of these issues, recent work has begun to explore alternative aqueous-based methods for functionalisation of biosensors [1]. The discussion here also illustrates the importance of considering each substance used when electrical characterising a device to verify if functionalisation has worked. The qualitative presence of a change in characteristics (or lack of one) over the full process is not sufficient to make conclusive remarks regarding successful functionalisation. A full set of electrical control measurements are required for an understanding of electronic changes occurring during the functionalisation process, in the manner of Besteman *et al.* [33].

1.3. Attachment of 1-Pyrenebutanoic Acid N-Hydroxysuccinimide Ester

Table 1.2.: Comparison of 1-pyrenebutanoic acid (PBA) functionalisation processes used for immobilisation of proteins, enzymes and aptamers onto carbon nanotubes and graphene. 1-ethyl-3-(3-dimethylaminopropyl) carbodiimide hydrochloride (EDC) and NHS were co-mingled in buffer/electrolyte solution or DI water in each process - some papers used N-hydroxysulfosuccinimide instead of N-hydroxysuccinimide, and both compounds are abbreviated as NHS in this table for simplicity. Device exposure times to each solution are shown next to the solution concentration. Blank entries indicate there was no mention of the parameter in a particular paper. [†]PEG or PEG pyrene were used to reduce non-specific binding. ^{††}Several pyrene-based linkers were compared and PBA gave an optimal functionalisation result.

Solvent	Channel	PBA (mM)	Time (hr)	EDC (mM)	NHS (mM)	Time (min)	References
DMF	Graphene	0.6	1	-	-	120	Gao, 2016 [†] . [63]
		5	2	2	5	30	Mishyn, 2022. [5]
	CNT	100	3	200	-	30	Min, 2012. [64]
	Graphene, CNT	7.6	2	8	20	120	Xu, 2014. [65]
DI water	CNT	-	-	32	12	Overnight	Pacios, 2012 [†] . [66]
Ethanol	CNT	1	1	100	100	20	Filipiak, 2018 [†] . [67]
Acetonitrile	Graphene	1	1	400	100	60	Tong, 2020 ^{††} . [9]
Borax	CNT	2	24	2.5	-	1080	Liu, 2011 [†] . [68]
DMSO	Graphene	5	1	50	50	90	Fenzl, 2017. [69]

1.4. Attachment of 1-Pyrenebutyric Acid

1.4.1. Comparing Attachment Methods

Another linker molecule that can be used to attach receptor molecules to a carbon nanotube or graphene channel is 1-pyrenebutyric acid (PBA or PyBA). As with PBASE, the pyrene group of PBA has a π interaction with the carbon rings of the channel surface. It is possible to react PBA with 1-ethyl-3-(3-dimethylaminopropyl) carbodiimide hydrochloride (EDC or EDAC) to form an *O*-acylisourea intermediate, which can then react with an amine group on a biomolecule and form an amide bond [70], [71]. The water solubility of EDC means that, unlike PBASE, it is possible to functionalise with EDC dissolved in water rather than in an organic solvent. However, like PBASE, EDC and the *O*-acylisourea intermediate are prone to hydrolysis, especially in acidic conditions. Therefore, like PBASE, it should be stored at -20°C , and warmed to room temperature to prevent condensation build-up, since exposure to condensation will hydrolyse the reagent [71]. Furthermore, by adding N-Hydroxysuccinimide (NHS) or N-hydroxysulfosuccinimide (sulfo-NHS) to the reaction vessel, PBASE is formed as an active intermediate, which is less prone to hydrolysis and increases the PBA/EDC reaction yield [70]–[72].

A full comparison of functionalisation procedures used for linking carbon nanotube and graphene devices to aptamers and proteins with PBA is given in Table 1.2. To the best of my knowledge, this table is as complete a summary as possible of 1-pyrenebutyric acid functionalisation processes for carbon nanotube and graphene field-effect transistor biochemical sensors. By comparing Table 1.1 and Table 1.2, it is clear that PBASE is more widely used for non-covalent functionalisation than PBA/EDC. As was the case for PBASE, there are a wide range of process variables used for the functionalisation process, with little justification used for variables chosen. Also notable is the frequent use of polyethylene glycol (PEG) or pyrene-PEG for prevention of non-specific binding (NSB). Non-specific binding is discussed further in [?@sec-non-specific-binding](#). Despite being less widely used, Mishyn *et al.* [5] state a preference for the use of PBA/EDC over PBASE, as they found it was less prone to hydrolysis and gave a larger reaction yield when binding ferrocene to graphene. A potential downside of using PBA/EDC for protein immobilisation is that EDC has numerous ways of interacting with proteins, and not all of these are necessarily desirable; furthermore, the addition of NHS may also cause other issues, such as precipitation of the reaction compound [71]. The greater range of process variables involved in the functionalisation also adds to the complexity of reproducing past results.

1.4.2. Raman Spectroscopy

Raman spectroscopy was used to verify the attachment of PBA to a carbon nanotube network film with a silicon dioxide substrate in the manner outlined in [?@sec-raman-](#)

1.4. Attachment of 1-Pyrenebutyric Acid

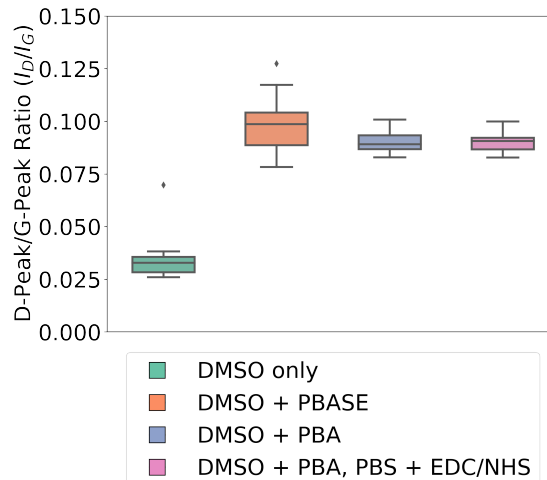


Figure 1.6.: This box plot shows the distribution of D-band peak to G^+ -band peak ratio, I_D/I_G , across nine locations for a selection of chemically-modified carbon nanotube films. The D-band and G-band intensities for all samples were first normalised to the intensity peak corresponding to the silicon dioxide substrate.

characterisation. As highly-bundled devices were found to have less defects present prior to modification, as discussed in ?@sec-pristine-raman, solvent-deposited films were used for the verification of pyrene attachment to prevent the initial presence of defects influencing the analysis. Droplets of DMSO solution were placed on three (solvent-deposited) carbon nanotube films taken from the same wafer. The DMSO solution on one film contained 5 mM PBA, the solution on another film contained 5 mM PBASE, and the DMSO on the final film contained no linker molecule. After incubation for 1 hour, films were rinsed for 15 s with DMSO, then for 15 s with IPA to remove excess DMSO while avoiding hydrolysis of the PBASE. After the first set of Raman spectra was taken, the film initially exposed to PBA was further exposed to a solution of 20 mM EDC and 40 mM NHS in 1× PBS electrolyte for 30 minutes, and a second set of Raman spectra was taken for this film. As in ?@sec-pristine-raman, two spectra taken at each position were processed according to Section B.3, and the silicon dioxide reference peak measured in the wavenumber range $100\text{ cm}^{-1} - 650\text{ cm}^{-1}$ was used to normalise the D-band and G-band peaks from the wavenumber range $1300\text{ cm}^{-1} - 1650\text{ cm}^{-1}$. The ratio between the average intensity of the D-peak and the G^+ -peak at each position was calculated, and the distribution of ratio values corresponding to each modified film is shown in Figure 1.6.

There is a $\sim 3\times$ increase in the intensity ratio I_D/I_G for both the films modified with PBASE and PBA compared to the film which was only exposed to DMSO. Previous works have found that a change in the intensity ratio indicates successful π -stacking on the carbon nanotube surface, as it indicates surface modification of the carbon nanotubes

1. Non-Covalent Functionalisation of Carbon Nanotube and Graphene Films

has occurred [73], [74]. Wei *et al.* [73] found functionalisation with PBASE altered the ratio by a factor of $\sim 1.5\times$, while Lan *et al.* [74] found that functionalisation with PBA altered the ratio by a factor of $\sim 0.8\times$. The reason for the large difference between results is not immediately clear, but may result from the significant differences in the pristine composition and morphology of carbon nanotube networks used in each publication, and differences in the functionalisation method used. Across all scan locations in ?@fig-raman-comparison, the value found for I_D/I_G is consistently ~ 0.095 for both PBA and PBASE. Furthermore, subsequent Raman measurements of the PBA-modified film after further functionalisation with EDC/NHS do not show a significant change in I_D/I_G . These results indicate that presence of the NHS ester has little effect on the Raman shift. It should be clarified that Raman spectroscopy cannot be used to distinguish between the presence of PBA and PBASE on the device surface. However, it is clear that functionalisation of the carbon nanotube network with both the PBA and PBASE has led to measurable *pi*-stacking between the network and the pyrene group attached to each compound.

1.4.3. Electrical Characterisation

Figure 1.7 shows the transfer characteristics of a carbon nanotube transistor channel at various stages of a PBA/EDC functionalisation, where a excess of N-hydroxysuccinimide (NHS) was added alongside EDC. A solvent-deposited carbon nanotube film was used for the device. The PBA was dissolved in DMSO, and the device channels were exposed to this solution for 1 hour. The electrical change resulting from PBA exposure is shown in Figure 1.7a. The threshold shift with the addition of 5 mM PBA in DMSO for 1 hour is equivalent to the shift seen when only DMSO is added, $\Delta V = -0.15$ V. The lack of a significant threshold shift directly attributable to the PBA is a result of pyrene having a neutral charge state; any contributions from the charged carboxyl group are screened from the carbon nanotube sidewalls by surrounding water molecules [75]. However, as in the case of the addition of PBASE, there also appears to be an increase in hole mobility, which may be due to the pyrene groups increasing connectivity within the carbon nanotube network [13].

Subsequently, the device was rinsed with 1× PBS and exposed to 20 mM EDC and 40 mM NHS in 1× PBS electrolyte for 30 minutes. Figure 1.7b shows the change resulting from subsequent EDC/NHS exposure. When EDC/NHS is added, a threshold shift of $\Delta V \sim -0.08$ V was observed on multiple channels. The exposure to EDC/NHS negatively shifts the transfer characteristic curve, most likely due to the PBA present reacting to form positively-charged *O*-acylisourea esters and negatively gating the attached carbon nanotube network [60], [71]. Figure 1.7c shows that this shift is not significantly affected by further exposure of the channel to PBS. The lack of a change in gating may imply that hydrolysis over the course of one hour is insufficient to hydrolyse a significant proportion of the attached *O*-acylisourea or PBASE back to PBA, leaving them available for reaction with biomolecule amine groups. A further test could be performed to see if leaving the

1.4. Attachment of 1-Pyrenebutyric Acid

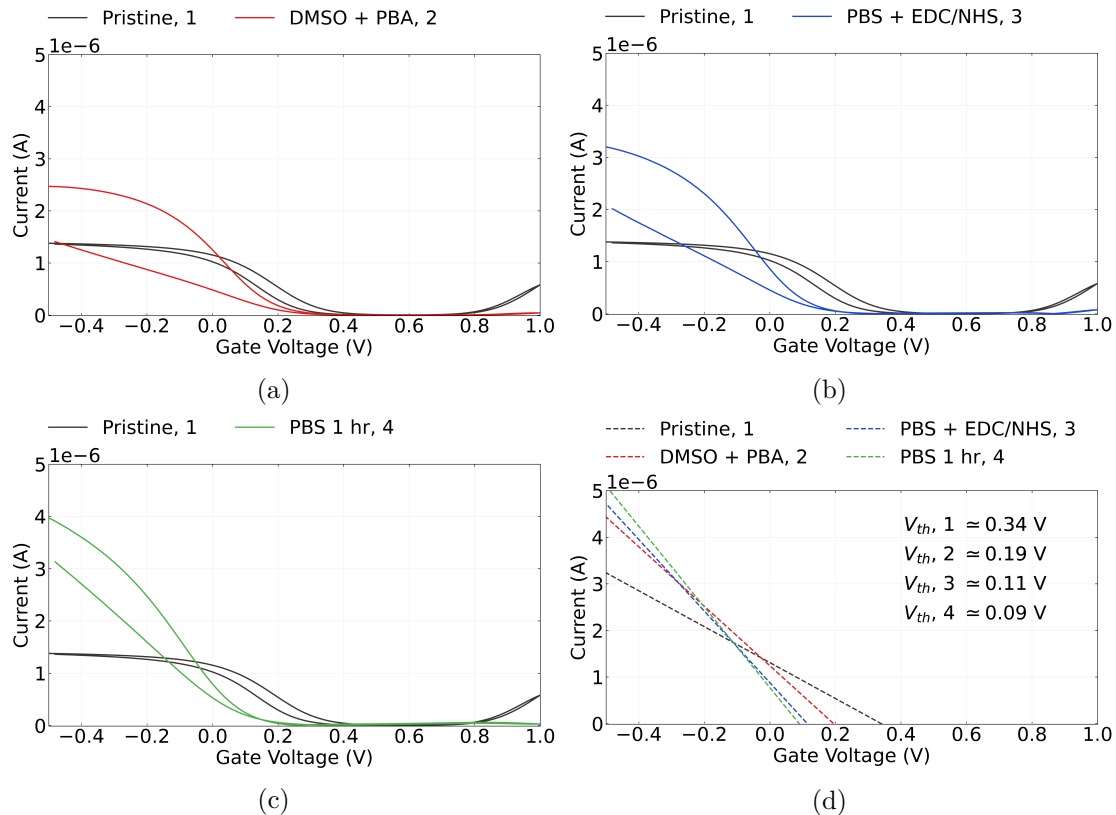


Figure 1.7.: Electrical transfer characteristics of a carbon nanotube transistor before functionalisation alongside the transfer characteristics (a) after being submerged in DMSO containing 5 mM PBA for 1 hour in red, (b) after being submerged in 1× PBS containing 20 mM EDC and 40 mM NHS for 30 min in blue, and (c) after being submerged in fresh 1× PBS for 1 hour in green. The dashed lines in (d) are linear fits tangent to the subthreshold slope of each characteristic curve, and are shown alongside the threshold voltages calculated by finding the intercept of each fit.

1. Non-Covalent Functionalisation of Carbon Nanotube and Graphene Films

device submerged in water over a longer time period to check if ester hydrolysis eventually affects threshold voltage in a significant manner, but this was considered to be outside the scope of this work.

1.5. Attachment of PEGylated Pyrene-Based Linkers

1.5.1. Pyrene-NTA, Pyrene-Biotin and PEGylation

Through chemical coupling/conjugation, it is possible to replace the NHS ester group on PBASE with other groups that can undergo binding reactions with proteins. Unlike PBASE, these groups do not suffer the drawback of being readily hydrolysed. For example, PBASE can be modified with $\text{N}\alpha,\text{N}\alpha\text{-Bis(carboxymethyl)-L-lysine}$ hydrate (also known as N-(5-Amino-1-carboxypentyl)iminodiacetic acid, AB-NTA) to produce pyrene-nitrilotriacetic acid (pyrene-NTA). The attached NTA group is able to chelate with metal ions such as Cu^{2+} or Ni^{2+} , which then can then coordinate with polyhistidine-tags attached to a protein [76]–[78]. Use of Cu^{2+} ions over Ni^{2+} gives stronger histidine bonding and less non-specific adsorption [78]. Functionalisation using the NTA- Ni^{2+} chemistry was successfully used to attach mammalian odorant receptors to a single carbon nanotube for detection of eugenol vapour in real-time [11]. Pyrene-biotin (pyrene butanol biotin ester) can also be produced for attaching avidin or streptavidin [76]. As avidin and streptavidin are tetrameric, they can be attached to both pyrene-biotin and biotinylated avi-tagged proteins simultaneously via strong non-covalent bonding, therefore linking the transducer and receptor [79]–[82]. As the presence of his-tags and avi-tags on proteins can be readily controlled, these methods offer improved specificity and directionality over the traditional amide bonding seen earlier.

It is also possible to attach polyethylene glycol (PEG) chains to a pyrene group and modify them with reactive groups such as NTA and biotin to attach proteins in the manner outlined in the previous paragraph [83], [84]. Once modified with PEG, the water solubility of pyrene linkers increases, making it possible to perform a full functionalisation procedure exclusively in aqueous solution [83]. By setting the length of the PEG chain, the size of the linker molecule can be controlled - selection of a short chain is important for ensuring attached receptors remain within the Debye length of the transducer [3]. Functionalisation of a graphene transducer with pyrene-PEG-biotin has previously been used to bind streptavidin to a graphene field-effect transistor device [85]. The PEGylated linkers used in the following sections were purchased pre-prepared. Pyrene-PEG-NTA (2 kDa) was purchased from Nanocs, while pyrene-PEG-FITC (2 kDa, 10 kDa), pyrene-PEG-rhodamine (3.4 kDa), mPEG-Pyrene (10 kDa) and pyrene-PEG-biotin (10 kDa) were purchased from Creative PEGworks.

1.6. Identifying Functionalisation Obstacles using Fluorescence Microscopy

1.6.1. General Overview

Various dyes and fluorescent tags were used to investigate approaches for identifying successful attachment of biomolecules to a carbon nanotube or graphene surface with fluorescence microscopy. The dyes included fluorescein isothiocyanate (FITC), Rhodamine B and Cyanine 3 (Cy3). Green fluorescent protein was also used for this testing process. It is important to note that these dyes and the GFP chromophore all contain benzene rings which are able to π -stack with carbon rings to some degree [86]–[89]. However, there is also significant variation in the effectiveness of this π -stacking, as shown by Figure 1.8. Here, a clear, specific interaction is seen between Rhodamine B and graphene, but little interaction between FITC and graphene is observed, even when a longer exposure time is used. Whether the addition of pyrene linker groups these dyes, or dye-modified biomolecules, was therefore investigated in further detail. This process then led to the identification of multiple issues that could impede a successful device functionalisation.

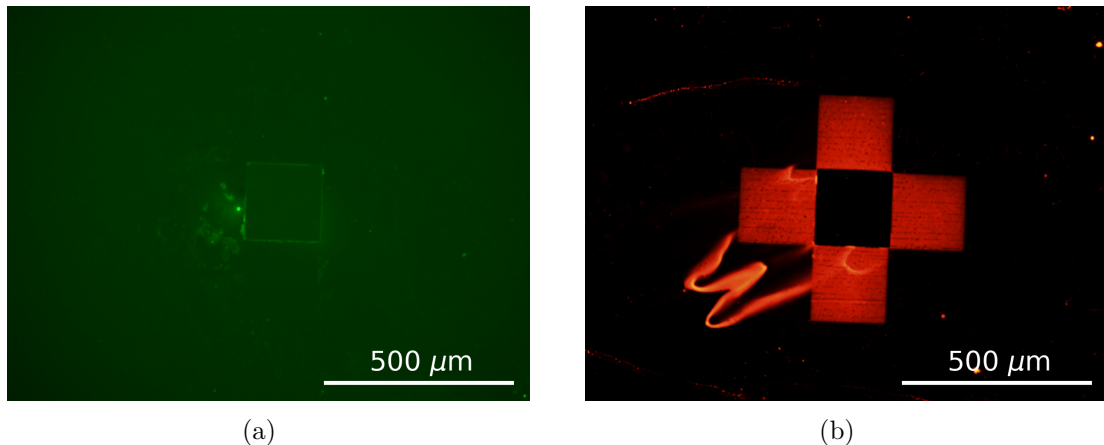


Figure 1.8.: Four 200 $\mu\text{m} \times 200 \mu\text{m}$ graphene squares modified with the dyes (a) fluorescein isothiocyanate (FITC) and (b) Rhodamine B. No pyrene/PEG/pyrene-PEG was attached to these dyes. In (a), an FITC filter and 6.5 s exposure time was used, and in (b) a Texas Red filter and 1.4 s exposure time was used.

Both SU8 and AZ® 1518 photoresist fluoresced under a variety of microscope filters, resulting from light interacting with the photoactive component present in both resists [90]. This background fluorescence was found to drown out fluorescence from a dye-functionalised device channel, and so photoresist encapsulated devices were not used for fluorescence imaging. (Consider a photograph of a dim outdoor lamp; if the photograph

1. Non-Covalent Functionalisation of Carbon Nanotube and Graphene Films

was taken on a starless night, the light from the lamp would show up clearly, but with the sun out the light would be very difficult to see regardless of how the photograph was taken.) A different type of encapsulation could potentially be used to verify linker attachment with fluorescence after a device has been encapsulated. These alternative encapsulation methods for use with fluorescence microscopy are discussed in [?@sec-future-work-fabrication](#).

1.6.2. Photoresist Contamination

An functionalisation issue quickly encountered when characterising pyrene-PEG-FITC (PPF) interaction with sensing channels via fluorescence microscopy was an unwanted secondary interaction between the linker and residual photoresist. Figure 1.9a and Figure 1.9b are fluorescence images of SU8 encapsulation (using the pre-2023 mask) before and after being exposed to PPF. Despite the same microscope settings being used to take the images (filter, ISO, contrast, exposure time), the SU8 exposed to PPF appears much brighter than the pristine SU8. This result indicates that the linker appears to have an extensive interaction with the photoresist via an unknown mechanism. No fluorescence is seen from the device channel. The length of exposure time required to see fluorescence from the modified channel would lead to fluorescence from the modified linker attached to the photoresist – as well as the photoresist itself – flooding the image with light. Therefore, it is not clear whether the carbon nanotubes have been functionalised with the dye-modified linker. However, out of caution we can assume that the presence of this secondary interaction is not desirable.

A similar interaction was seen between AZ® 1518 photoresist and fluorescent-tagged, amine-terminated aptamer. An unencapsulated carbon nanotube network device, fabricated using the pre-June 2022 process outlined in [?@sec-fabrication](#), was incubated with 500 nM Cy3-tagged aptamer in Tris buffer at 4°C overnight. The aptamer was first denatured by heating in a water bath at 95°C for 5 minutes then cooling in an ice bath for 10 minutes before use.

Figure 1.9c and Figure 1.9d are fluorescence images of the device channel region before and after exposure to aptamer. A thick red ring is visible around the electrodes after functionalisation, despite no PBASE being used to tether the amine-terminated aptamer. It appears that these bright patches correspond to patches of residual photoresist which have not been completely removed from the carbon nanotube square by the development process. These patches have then interacted with the aptamer, causing them to appear bright under the fluorescence microscope. Beyond potentially interfering with functionalisation, photoresist residue blocking a device channel will prevent interaction with the buffer and prevent sensing.

To test whether residual resist could be prevented from interacting with aptamer by crosslinking the resist, two unencapsulated devices were prepared as follows. Devices were first spincoated with AZ® 1518 in the manner described in [?@sec-fabrication](#).

1.6. Identifying Functionalisation Obstacles using Fluorescence Microscopy

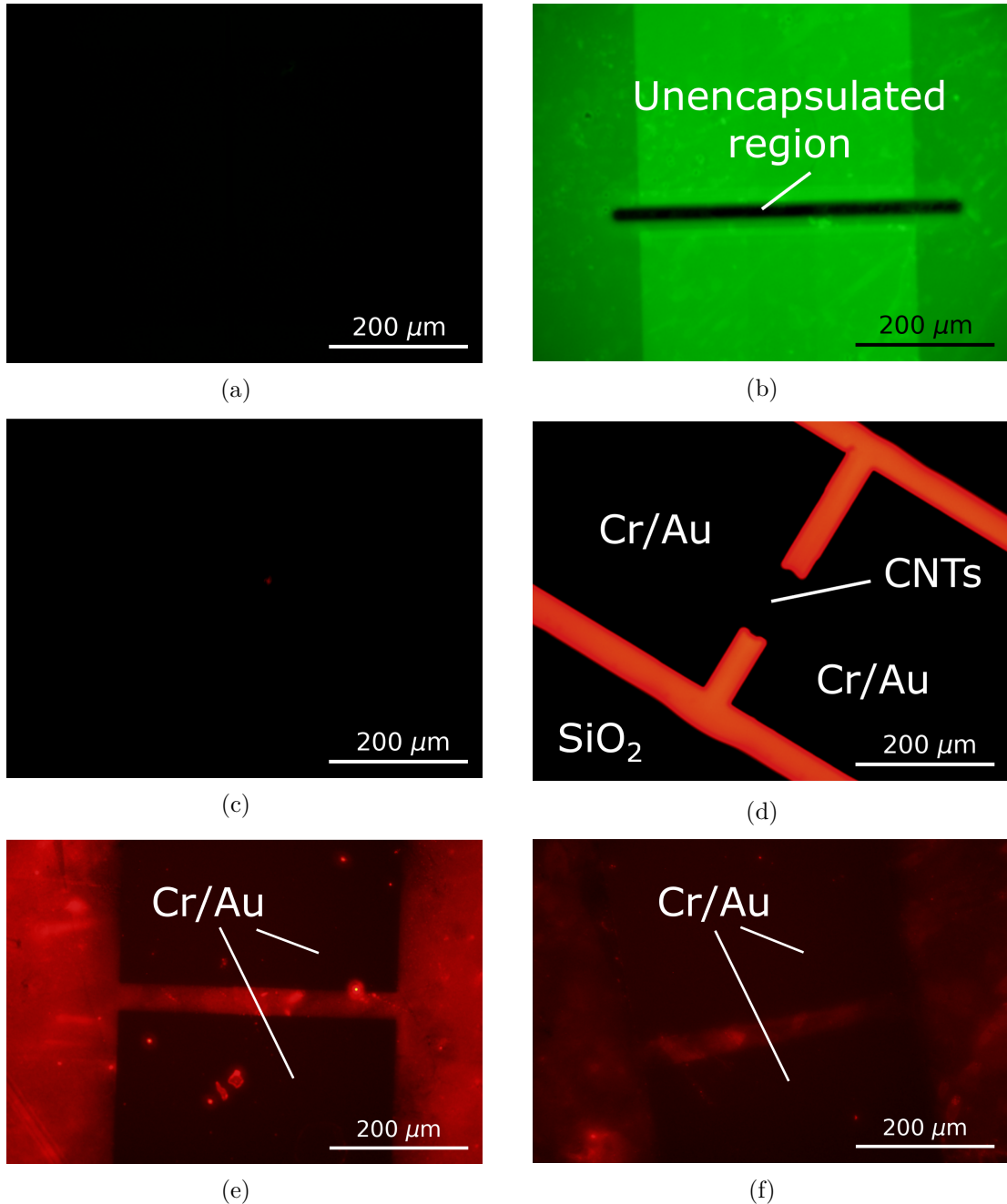


Figure 1.9.: A fluorescence image of a SU8-encapsulated carbon nanotube device is shown in (a), while (b) shows the same channel after modification with a solution of 1 mM Pyrene-PEG-FITC. A 0.35 s exposure time and FITC filter were used for (a)-(b). The fluorescence image in (c) shows an unencapsulated channel, while (d) shows the same channel after Cy3-tagged aptamer exposure. A 10 s exposure time and mCherry filter were used for (c)-(d). The fluorescence images in (e) and (f) show devices pre-coated with a thin layer of photoresist then submerged in Cy3-tagged aptamer, where the device in (f) was hardbaked before aptamer exposure. An mCherry filter and 30 s exposure time were used for (e)-(f).

1. Non-Covalent Functionalisation of Carbon Nanotube and Graphene Films

Next, the majority of resist was removed by soaking the device in acetone for 1 minute. This process left a thin coating of photoresist on the devices. One of these devices was then hardbaked at 200°C for 1 hour. Both devices were subsequently functionalised in the following manner:

1. Unencapsulated device was submerged in 1 mM PBASE in methanol solution for 1 hour.
2. The device was then rinsed with methanol and Tris buffer.
3. 1 µM Cy3-tagged aptamer was denatured by heating in a water bath at 95°C for 5 minutes then cooling in an ice bath for 10 minutes before use.
4. The device was incubated with aptamer in Tris buffer at 4°C overnight.

Fluorescence microscope images of channels from each device are shown in Figure 1.9e and Figure 1.9f, where the latter is the device hardbaked before functionalisation. By comparing the two images, it is apparent that hardbaking the AZ® 1518 photoresist significantly reduces the amount of fluorescent aptamer attached to the surface. This result is an indication that sufficient heating of the photoresist can prevent it interacting with PBASE or amine-tagged biological material. However, there is still some Cy3-tagged aptamer fluorescence visible in Figure 1.9f. It appears that hardbaking has not completely prevented photoresist from interacting with the aptamer. It is possible that heating from the bottom of the device is insufficient to hardbake the photoresist layer completely, an effect that would be amplified for the thick photoresist layer on encapsulated devices. Therefore, from June 2023 onwards devices were vacuum annealed for 1 hour at 150°C prior to functionalisation. This approach was taken to ensure photoresist was heated from above as well as below and made chemically inert across its surface.

This result demonstrates the use of fluorescence microscopy as a tool to detect residue and test suitable residue elimination measures. Further testing showed that performing a 1 minute flood exposure (for positive resist only) then placing a device in AZ® 326 developer for 3 minutes was highly effective at removing photoresist residue. Both these development and annealing techniques were used for all functionalised devices in subsequent sections.

1.6.3. Hydrophobicity of Carbon Nanotubes and Graphene

As PEGylated linker dissolves well in aqueous solution, initial fluorescence imaging focused on functionalising devices with these linkers dissolved in 1× PBS. It was hoped that by keeping the device channels in a pH-controlled environment, the channel surface would be made more suitable for the attached receptors. Figure 1.10a shows a graphene film after exposure to pyrene-PEG-rhodamine (PPR) in 1× PBS solution for 1 hour. The pyrene-PEG-rhodamine has interacted with the silicon dioxide substrate (discussed

1.6. Identifying Functionalisation Obstacles using Fluorescence Microscopy

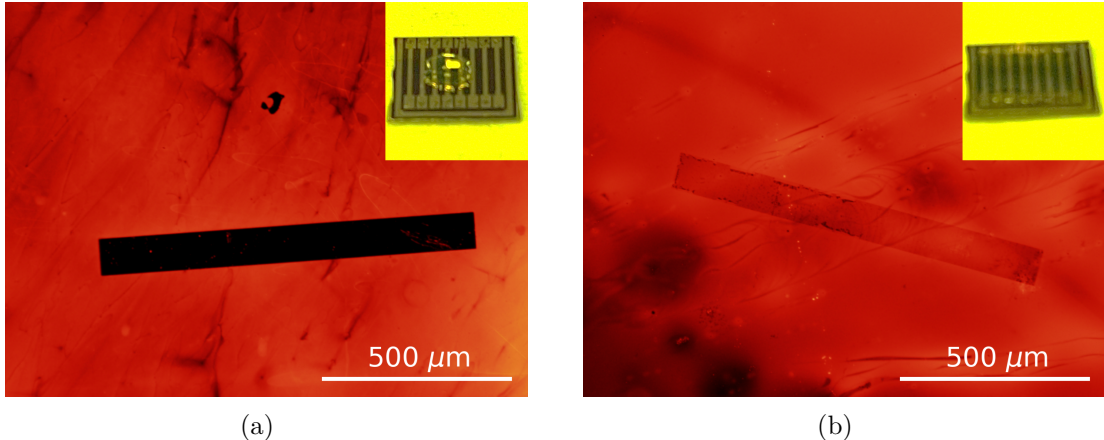


Figure 1.10.: Fluorescence images of a $1000 \mu\text{m} \times 100 \mu\text{m}$ graphene channel after functionalisation with 1 mM pyrene-PEG-rhodamine in $1\times$ PBS. The graphene film in (a) was not oxygen plasma cleaned before functionalisation, while the graphene film in (b) was oxygen plasma cleaned at 5 W for 15 s at 300 mTorr pressure immediately before functionalisation. Insets show a $10 \mu\text{L}$ droplet placed on an unencapsulated carbon nanotube device before (a) and after (b) the same oxygen plasma treatment procedure. Images were taken using a Texas Red filter and a 1.8 s exposure time.

further in Section 1.6.4) but not the graphene film. The graphene has not attached to the pyrene or rhodamine due to the highly hydrophobic graphene surface repelling the surrounding solution, preventing π -stacking from occurring. The hydrophobicity of the graphene surface is not intrinsic to graphene. Instead, it results from a hydrocarbon layer which forms on the channel surface when exposed to air, primarily composed of long-chain alkanes [91], [92]. A hydrophobic layer will also form on carbon nanotube networks [93], [94]. Treatment with oxygen plasma at 5 W for 15 s has previously been found to remove this hydrocarbon layer, restoring the intrinsic hydrophilicity of graphene [95]. Storing the graphene surface in deionised water rather than air prevents the return of this hydrocarbon layer [91]. The use of a relatively low power plasma ensures damage to the graphene layer is minimised.

Treatment of an unencapsulated carbon nanotube network device at 5 W for 15 s at 300 mTorr greatly reduced the contact angle of a water droplet placed on the device surface, shown inset in Figure 1.10 before and after plasma treatment. A graphene film was then functionalised with pyrene-PEG-rhodamine in $1\times$ PBS in the same manner as for the film in Figure 1.10a, except with the same plasma treatment performed on the film less than 1 minute before functionalisation. The result is shown in Figure 1.10b. The graphene now appears to interact with the pyrene-PEG-rhodamine. These results both indicate that the plasma treatment is increasing the hydrophilicity of the device surface, improving the ability of pyrene-PEG-rhodamine to π -stack with graphene. The disadvantage of this procedure is that the plasma cleaning introduces defects to the graphene surface which

1. Non-Covalent Functionalisation of Carbon Nanotube and Graphene Films

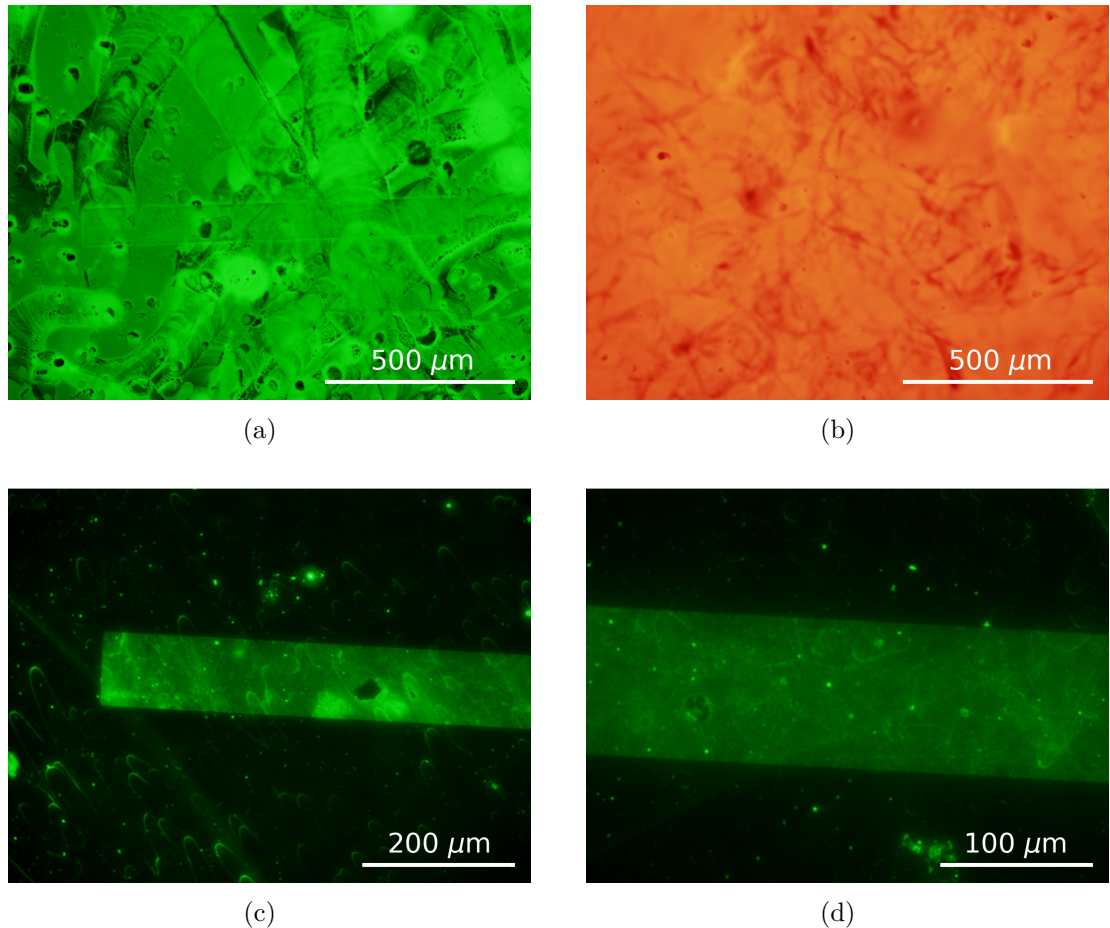


Figure 1.11.: The $1000 \mu\text{m} \times 100 \mu\text{m}$ graphene film in image (a) was functionalised with 1 mM pyrene-PEG-FITC in $1\times$ PBS after oxygen plasma treatment, taken using an FITC filter and a 1.6 s exposure time. (b) shows a silicon dioxide surface which had never been exposed to carbon nanotubes, graphene or photoresist after exposure to 1 mM pyrene-PEG-rhodamine in $1\times$ PBS, taken using a Texas Red filter and a 1.8 s exposure time. Graphene films on a substrate functionalised with 1 mM pyrene-PEG-FITC in $1\times$ PBS after oxygen plasma treatment then cleaned with m-CNT dispersion surfactant (NanoIntegris) are shown in (c) and (d), where a FITC filter was used, with 7.5 s and 7.75 s exposure times respectively.

1.6. Identifying Functionalisation Obstacles using Fluorescence Microscopy

may be undesirable for device electrical behaviour. Furthermore, it was often found that devices functionalised in this manner had their conductance drop significantly after functionalisation, even though plasma treatment itself did not significantly alter device conductance. Solvent was therefore used for the initial linker functionalisation in **?@sec-linker-receptor-attachment**, as it did not require a plasma cleaning step for successful attachment.

1.6.4. Substrate Interaction with Linker Molecules

Another issue that arose when verifying surface functionalisation was the interaction between pyrene linker and the silicon dioxide substrate. This interaction meant it was difficult to discern whether the pyrene group was interacting in a specific manner with the channel film. It was confirmed that pyrene-PEG was interacting with silicon dioxide, rather than residual photoresist or nanomaterial, by performing a pyrene-PEG-rhodamine functionalisation on pristine silicon dioxide, as shown in Figure 1.11b. The PEGlyated linker supplier suggested that the surface should be thoroughly rinsed with surfactant to remove weakly-bound pyrene-PEG-FITC attached to the silicon dioxide, while preserving the pyrene-PEG-FITC strongly attached via π -stacking to the graphene or carbon nanotube film [96]. The following process was then used to remove pyrene-PEG-FITC from the silicon dioxide: the film was rinsed with DI water for 30 s, then placed in m-CNT dispersion solution (NanoIntegris) for 5 minutes at 70°C while agitating with a pipette, and finally rinsed with DI water, ethanol, acetone, IPA and nitrogen dried. The results of this thorough cleaning process are shown in Figure 1.11c and Figure 1.11d. The majority of pyrene-PEG-FITC was removed in regions with no graphene, but remained where graphene was present, indicating specific, π -stacking interaction took place between the pyrene-PEG-FITC and graphene. However, this surfactant rinse step was not used when performing functionalisation with biological materials, to prevent damage to the lipid membranes used.

1.6.5. Coffee-Ring Effect

From Table 1.1, full device submersion appears to be the most common approach for functionalisation with solution containing linker molecules like PBASE. However, some groups placed small droplets of solution onto the device channels when functionalisation, and this approach was tested as part of the fluorescence verification work. For functionalisation with his-tagged green fluorescent protein, after plasma cleaning at 5 W for 15 s at 300 mTorr, a 4 μ L droplet of 100 μ M pyrene-PEG-NTA in 1 \times PBS was placed on each graphene device channel and left covered in a humid environment for 15 minutes. The device was then rinsed with 1 \times PBS, submerged in 10 mM NiSO₄ in 1 \times PBS for 1 hour, rinsed in 1 \times PBS, then submerged in 10 mL of 100 ng/mL his-tag GFP solution (Thermofisher) overnight. Fluorescence microscope imaging showed that a ring

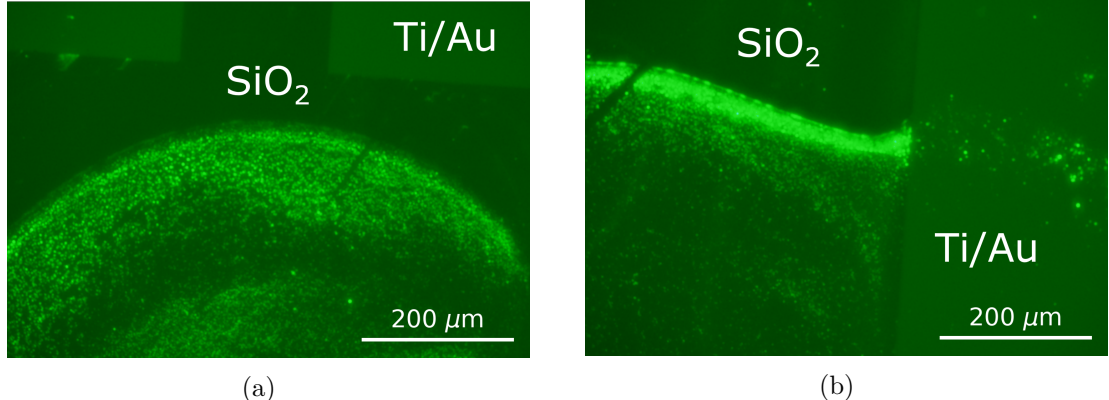


Figure 1.12.: Both (a) and (b) show a build-up of his-tag GFP at the edges of the droplet region where pyrene-PEG-NTA had been present, taken using an GFP filter and a 5 s exposure time. On the right hand side of (b), no his-tag GFP is visible on the metal electrode, as no pyrene-PEG attaches to the metal electrodes.

of biomaterial would build up around the outer edge of regions where pyrene-PEG-NTA had been present, as seen in Figure 1.12.

It appears this is a result of the his-tag GFP attaching to a dense region of pyrene-PEG-NTA at the edge of the functionalisation droplet. This accretion of pyrene-PEG-NTA at the edge of the droplet is a result of the coffee-ring effect, where the evaporation of the droplet leads to transport of particles to the droplet edges via capillary flow [97], [98]. As this gradient in surface coverage of attached proteins has unknown consequences for sensing, in the subsequent chapter devices were always functionalised by submerging them in solution instead of dropcasting.

1.7. Conclusion

It has been well-established in the literature that the π -stacking reaction mechanism between pyrene-based linkers and graphene and carbon nanotube network field-effect transistors can be used to create working biosensors. The previous use of various linker molecules for biosensor functionalisation was investigated. Despite the wide use of 1-pyrenebutanoic acid N-hydroxysuccinimide ester (PBASE) and 1-pyrenebutyric acid (PBA) for functionalisation of biosensors, the literature shows a significant variation in the methods used for attachment of linker molecules to a transistor channel. The most common methods, using 6 mM PBASE dissolved in dimethylformamide or 1 mM PBASE in methanol, stem directly from the first documented use of PBASE for functionalisation of carbon nanotube biosensors. In the last 6 years, more research has been

1.7. Conclusion

done into optimising the PBASE methodology for graphene devices, but there is still disagreement in the literature over whether minimising or maximising PBASE coverage on a graphene device channel is desirable for sensing. Due to disagreement in the literature around suitable non-covalent methods for biosensor functionalisation, several steps were taken to identify a rapid and simple method for verifying successful functionalisation, and to locate any potential barriers to a successful functionalisation.

I first compared the advantages and disadvantages of the various linker molecules under investigation. The use of hydrogen NMR gave indications that water was present in PBASE samples prepared in DMSO. Concerns around the impact of the hydrolysis of PBASE on functionalisation mean that the presence of water is strongly undesirable. An alternative functionalisation approach less prone to hydrolysis is the reaction of PBA with EDC in the presence of NHS. However, this process has its own disadvantages, such as undesirable protein interactions and the increased amount of steps and process variables involved. Pyrene-NTA is also less prone to hydrolysis than PBASE but unlike PBASE or PBA/EDC interacts with a specific protein tag, the histidine tag. PEGylation of the pyrene-NTA linker also means that the entire functionalisation process can be performed in aqueous solution, avoiding the introduction of non-organic solvents. This approach is desirable, since the non-aqueous solvents traditionally used for functionalisation may have negative impacts on device behaviour. For example, carbon nanotube device channel transfer characteristics were found to undergo a significant shift of $\Delta V = -0.15 \pm 0.02$ when exposed to DMSO or MeOH for 1 hour.

Next, I verified that the pyrene groups of the linker molecules of interest were attaching successfully to either carbon nanotubes or graphene. Raman spectroscopy showed that incubating a highly-bundled carbon nanotube film in 5 mM PBASE or PBA in DMSO for 1 hour increased I_D/I_G by a factor of ~ 3 relative to the DMSO-only case. Incubating a steam-deposited carbon nanotube device in a 1 mM concentration of PBASE in methanol or DMSO for 1 hour was found to cause a significant increase in device on-current relative to the solvent-only case, and a similar increase in on-current was seen for 5 mM PBA in DMSO relative to the DMSO-only case. When a PBA-functionalised device was placed in aqueous solution with 20 mM EDC and 40 mM NHS for 30 minutes, a further increase in on-current was seen. Fluorescence microscopy was used to demonstrate the successful attachment of pyrene-PEG to graphene using an attached FITC probe, where immersing a graphene film in 1 mM pyrene-PEG in ethanol led to the channels becoming brightly fluorescent relative to the background using a 1 s exposure time.

Various obstacles to successful functionalisation were also encountered and addressed using fluorescence microscopy. Photoresist contamination was addressed with exposure and development steps before functionalisation (no exposure for SU8 encapsulated devices). Hydrophobicity of graphene films was addressed by plasma treatment before functionalisation in aqueous solution. A surfactant rinse was used to distinguish between weak substrate-linker interaction and π -stacking between linker and the channel. Finally, coffee-ring distribution of linker was addressed by always submerging the device in linker when functionalising.

A. Vapour System Hardware

Table A.1.: Major components used in construction of the vapour delivery system described in this thesis.

Description	Part No.	Manufacturer
Mass flow controller, 20 sccm full scale	GE50A013201SBV020	MKS Instruments
Mass flow controller, 200 sccm full scale	GE50A013202SBV020	MKS Instruments
Mass flow controller, 500 sccm full scale	FC-2901V	Tylan
Analogue flowmeter, 240 sccm max. flow	116261-30	Dwyer
Micro diaphragm pump	P200-B3C5V-35000	Xavitech
Analogue flow controller, for micro diaphragm pump	X3000450	Xavitech
10 mL Schott bottle	218010802	Duran
PTFE connection cap system	Z742273	Duran
Baseline VOC-TRAQ flow cell, red	043-951	Mocon
Humidity and temperature sensor	T9602	Telaire
Enclosure, for humidity and temperature sensor	MC001189	Multicomp Pro

B. Python Code for Data Analysis

B.1. Code Repository

The code used for general analysis of field-effect transistor devices in this thesis was written with Python 3.8.8. Contributors to the code used include Erica Cassie, Erica Happe, Marissa Dierkes and Leo Browning. The code is located on GitHub and the research group OneDrive, and is available on request.

B.2. Atomic Force Microscope Histogram Analysis

The purpose of this code is to analyse atomic force microscope (AFM) images of carbon nanotube networks in .xyz format taken using an atomic force microscope and processed in Gwyddion (see [?@sec-afm-characterisation](#)). It was originally designed by Erica Happe in Matlab, and adapted by Marissa Dierkes and myself for use in Python. The code imports the .xyz data and sorts it into bins 0.15 nm in size for processing. To perform skew-normal distribution fits, both *scipy.optimize.curve_fit* and *scipy.stats.skewnorm* modules are used in this code.

B.3. Raman Spectroscopy Analysis

The purpose of this code is to analyse a series of Raman spectra taken at different points on a single film (see [?@sec-raman-characterisation](#)). Data is imported in a series of tab-delimited text files, with the low wavenumber spectrum ($100\text{ cm}^{-1} - 650\text{ cm}^{-1}$) and high wavenumber spectrum ($1300\text{ cm}^{-1} - 1650\text{ cm}^{-1}$) imported in separate datafiles for each scan location.

B.4. Field-Effect Transistor Analysis

The purpose of this code is to analyse electrical measurements taken of field-effect transistor (FET) devices. Electrical measurements were either taken from the Keysight 4156C Semiconductor Parameter Analyser, National Instruments NI-PXIe or Keysight B1500A Semiconductor Device Analyser as discussed in [?@sec-electrical-characterisation](#);

B. Python Code for Data Analysis

the code is able to analyse data in .csv format taken from all three measurement setups. The main Python file in the code base consists of three related but independent modules: the first analyses and plots sensing data from the FET devices, the second analyses and plots transfer characteristics from channels across a device, and the third compares individual channel characteristics before and after a modification or after each of several modifications. The code base also features a separate config file and style sheet which govern the behaviour of the main code. The code base was designed collaboratively by myself and Erica Cassie over GitHub using the Sourcetree Git GUI.

Bibliography

- [1] Niazul I. Khan and Edward Song. "Detection of an IL-6 Biomarker Using a GFET Platform Developed with a Facile Organic Solvent-Free Aptamer Immobilization Approach". In: *Sensors 2021*, Vol. 21, Page 1335 21.4 (Feb. 2021), p. 1335. ISSN: 1424-8220. DOI: 10.3390/S21041335. URL: <https://www.mdpi.com/1424-8220/21/4/1335>.
- [2] Hong Phan T. Nguyen, Thanihaichelvan Murugathas, and Natalie O.V. Plank. "Comparison of Duplex and Quadruplex Folding Structure Adenosine Aptamers for Carbon Nanotube Field Effect Transistor Aptasensors". In: *Nanomaterials (Basel, Switzerland)* 11.9 (Sept. 2021). ISSN: 2079-4991. DOI: 10.3390/NANO11092280. URL: <https://pubmed.ncbi.nlm.nih.gov/34578596/>.
- [3] Bajramshahe Shkodra, Mattia Petrelli, Martina Aurora Costa Angeli, et al. "Electrolyte-gated carbon nanotube field-effect transistor-based biosensors: Principles and applications". In: *Applied Physics Reviews* 8.4 (Dec. 2021), p. 41325. ISSN: 19319401. DOI: 10.1063/5.0058591. URL: [/aip/apr/article/8/4/041325/1076095/Electrolyte-gated-carbon-nanotube-field-effect](https://aip.org/aip/apr/article/8/4/041325/1076095/Electrolyte-gated-carbon-nanotube-field-effect).
- [4] Nikita Nekrasov, Natalya Yakunina, Averyan V. Pushkarev, et al. "Spectral-phase interferometry detection of ochratoxin a via aptamer-functionalized graphene coated glass". In: *Nanomaterials* 11.1 (Jan. 2021), pp. 1–10. ISSN: 20794991. DOI: 10.3390/nano11010226. URL: <https://www.mdpi.com/2079-4991/11/1/226>.
- [5] Vladyslav Mishyn, Adrien Hugo, Teresa Rodrigues, et al. "The holy grail of pyrene-based surface ligands on the sensitivity of graphene-based field effect transistors". In: *Sensors and Diagnostics* 1.2 (Mar. 2022), pp. 235–244. ISSN: 2635-0998. DOI: 10.1039/D1SD00036E. URL: <https://pubs.rsc.org/en/content/articlehtml/2022/sd/d1sd00036e> %20https://pubs.rsc.org/en/content/articlelanding/2022/sd/d1sd00036e.
- [6] Erica Cassie, Hamish Dunham, Erica Happe, et al. "A comparison between oestradiol aptamers as receptors in CNT FET biosensors". In: *Sensors and Diagnostics* 2.6 (Nov. 2023), pp. 1561–1573. ISSN: 2635-0998. DOI: 10.1039/D3SD00055A. URL: <https://pubs.rsc.org/en/content/articlehtml/2023/sd/d3sd00055a> %20https://pubs.rsc.org/en/content/articlelanding/2023/sd/d3sd00055a.

Bibliography

- [7] Mitchell B. Lerner, Felipe Matsunaga, Gang Hee Han, et al. “Scalable production of highly sensitive nanosensors based on graphene functionalized with a designed G protein-coupled receptor”. In: *Nano Letters* 14.5 (May 2014), pp. 2709–2714. ISSN: 15306992. DOI: 10.1021/NL5006349/SUPPL_FILE/NL5006349_SI_001.PDF. URL: <https://pubs.acs.org/doi/full/10.1021/nl5006349>.
- [8] Sae Ryun Ahn, Ji Hyun An, Seung Hwan Lee, et al. “Peptide hormone sensors using human hormone receptor-carrying nanovesicles and graphene FETs”. In: *Scientific reports* 10.1 (Dec. 2020). ISSN: 2045-2322. DOI: 10.1038/S41598-019-57339-1. URL: <https://pubmed.ncbi.nlm.nih.gov/31942024/>.
- [9] Jing Tong, Lei Zhang, Yi Wang, et al. “High response photodetection by applying the optimized photoreceptor protein modification on graphene based field effect transistors”. In: *FrMat* 7 (July 2020), p. 222. ISSN: 22968016. DOI: 10.3389/FMATS.2020.00222. URL: <https://ui.adsabs.harvard.edu/abs/2020FrMat...7.222T/abstract>.
- [10] Shiyu Wang, Md Zakir Hossain, Kazuo Shinozuka, et al. “Graphene field-effect transistor biosensor for detection of biotin with ultrahigh sensitivity and specificity”. In: *Biosensors and Bioelectronics* 165 (Oct. 2020), p. 112363. ISSN: 18734235. DOI: 10.1016/J.BIOS.2020.112363. URL: [/pmc/articles/PMC7272179/](https://pmc/articles/PMC7272179/)?report=abstract%20https://www.ncbi.nlm.nih.gov/pmc/articles/PMC7272179/.
- [11] Brett R. Goldsmith, Joseph J. Mitala, Jesusa Josue, et al. “Biomimetic chemical sensors using nanoelectronic readout of olfactory receptor proteins”. In: *ACS Nano* 5.7 (July 2011), pp. 5408–5416. ISSN: 19360851. DOI: 10.1021/NN200489J/SUPPL_FILE/NN200489J_SI_001.PDF. URL: <https://pubs.acs.org/doi/full/10.1021/nn200489j>.
- [12] Minju Lee, Heehong Yang, Daesan Kim, et al. “Human-like smelling of a rose scent using an olfactory receptor nanodisc-based bioelectronic nose”. In: 8.1 (2018), pp. 1–12. ISSN: 2045-2322. URL: <https://www.nature.com/articles/s41598-018-32155-1%20https://pubmed.ncbi.nlm.nih.gov/30224633/>.
- [13] Thanihaichelvan Murugathas, Han Yue Zheng, Damon Colbert, et al. “Biosensing with Insect Odorant Receptor Nanodiscs and Carbon Nanotube Field-Effect Transistors”. In: *ACS Applied Materials and Interfaces* 11.9 (Mar. 2019), pp. 9530–9538. ISSN: 19448252. DOI: 10.1021/ACSAMI.8B19433. URL: <https://pubs.acs.org/doi/full/10.1021/acsami.8b19433>.
- [14] Thanihaichelvan Murugathas, Cyril Hamiaux, Damon Colbert, et al. “Evaluating insect odorant receptor display formats for biosensing using graphene field effect transistors”. In: *ACS Applied Electronic Materials* 2.11 (Nov. 2020), pp. 3610–3617. ISSN: 26376113. DOI: 10.1021/ACSAELM.0C00677. URL: <https://pubs.acs.org/doi/full/10.1021/acsaelm.0c00677>.

- [15] Dongseok Moon, Yeon Kyung Cha, So ong Kim, et al. “FET-based nanobiosensors for the detection of smell and taste”. In: *Science China. Life sciences* 63.8 (Aug. 2020), pp. 1159–1167. ISSN: 1869-1889. DOI: 10.1007/S11427-019-1571-8. URL: <https://pubmed.ncbi.nlm.nih.gov/31974862/>.
- [16] Jin Yoo, Daesan Kim, Heehong Yang, et al. “Olfactory receptor-based CNT-FET sensor for the detection of DMMP as a simulant of sarin”. In: *Sensors and Actuators B: Chemical* 354 (Mar. 2022), p. 131188. ISSN: 0925-4005. DOI: 10.1016/J.SNB.2021.131188.
- [17] Qing Cao and John A. Rogers. “Ultrathin Films of Single-Walled Carbon Nanotubes for Electronics and Sensors: A Review of Fundamental and Applied Aspects”. In: *Advanced Materials* 21.1 (Jan. 2009), pp. 29–53. ISSN: 1521-4095. DOI: 10.1002 / ADMA . 200801995. URL: <https://onlinelibrary.wiley.com/doi/full/10.1002/adma.200801995> % 20<https://onlinelibrary.wiley.com/doi/abs/10.1002/adma.200801995>.
- [18] Antonello Di Crescenzo, Valeria Ettorre, and Antonella Fontana. “Non-covalent and reversible functionalization of carbon nanotubes”. In: *Beilstein Journal of Nanotechnology* 5.1 (2014), p. 1675. ISSN: 21904286. DOI: 10.3762/BJNANO.5.178. URL: [/pmc/articles/PMC4222398/](https://pmc/articles/PMC4222398/) % 20[https://www.ncbi.nlm.nih.gov/pmc/articles/PMC4222398/](https://pmc/articles/PMC4222398/?report=abstract).
- [19] Xuesong Yao, Yalei Zhang, Wanlin Jin, et al. “Carbon Nanotube Field-Effect Transistor-Based Chemical and Biological Sensors”. In: *Sensors 2021, Vol. 21, Page 995* 21.3 (Feb. 2021), p. 995. ISSN: 1424-8220. DOI: 10.3390/S21030995. URL: <https://www.mdpi.com/1424-8220/21/3/995> % 20<https://www.mdpi.com/1424-8220/21/3/995>.
- [20] Kishan Thodkar, Pierre Andre Cazade, Frank Bergmann, et al. “Self-assembled pyrene stacks and peptide monolayers tune the electronic properties of functionalized electrolyte-gated graphene field-effect transistors”. In: *ACS Applied Materials and Interfaces* 13.7 (Feb. 2021), pp. 9134–9142. ISSN: 19448252. DOI: 10.1021/ACSAMI.0C18485/ASSET/IMAGES/LARGE/AM0C18485_0006.JPG. URL: <https://pubs.acs.org/doi/full/10.1021/acsami.0c18485>.
- [21] Chelsea R. Martinez and Brent L. Iverson. “Rethinking the term “pi-stacking””. In: *Chemical Science* 3.7 (June 2012), pp. 2191–2201. ISSN: 2041-6539. DOI: 10.1039/C2SC20045G. URL: <https://pubs.rsc.org/en/content/articlehtml/2012/sc/c2sc20045g> % 20<https://pubs.rsc.org/en/content/articlelanding/2012/sc/c2sc20045g>.
- [22] Emilio M. Pérez and Nazario Martín. “ $\pi-\pi$ interactions in carbon nanostructures”. In: *Chemical Society Reviews* 44.18 (Sept. 2015), pp. 6425–6433. ISSN: 1460-4744. DOI: 10.1039/C5CS00578G. URL: <https://pubs.rsc.org/en/content/articlehtml/2015/cs/c5cs00578g> % 20<https://pubs.rsc.org/en/content/articlelanding/2015/cs/c5cs00578g>.

Bibliography

- [23] Greg T. Hermanson. “Buckyballs, Fullerenes, and Carbon Nanotubes”. In: *Bioconjugate Techniques* (Jan. 2013), pp. 741–755. DOI: 10.1016/B978-0-12-382239-0.00016-9.
- [24] Yan Zhou, Yi Fang, and Ramaraja P. Ramasamy. “Non-Covalent Functionalization of Carbon Nanotubes for Electrochemical Biosensor Development”. In: *Sensors (Basel, Switzerland)* 19.2 (Jan. 2019). ISSN: 1424-8220. DOI: 10.3390/S19020392. URL: <https://pubmed.ncbi.nlm.nih.gov/30669367/>.
- [25] Carbonnanotube. *File:Noncovalent carboncarbonnanotube.png*. 2015. URL: https://en.m.wikipedia.org/wiki/File:Noncovalent_carboncarbonnanotube.png % 20<https://creativecommons.org/licenses/by/4.0/legalcode> (visited on 2023-10-13).
- [26] J. A. M. J. Frisch and G. W. Trucks and H. B. Schlegel and G. E. Scuseria and M. A. Robb and J. R. Cheeseman and G. Scalmani and V. Barone and G. A. Petersson and H. Nakatsuji and X. Li and M. Caricato and A. V. Marenich and J. Bloino and B. G. Janesko and R. G, J. E. Peralta, F. Ogliaro, et al. *Gaussian^16 Revision C.01*. 2016.
- [27] Yasuhiro Oishi, Hirotugu Ogi, Satoshi Hagiwara, et al. “Theoretical Analysis on the Stability of 1-Pyrenebutanoic Acid Succinimidyl Ester Adsorbed on Graphene”. In: *ACS Omega* 7.35 (Sept. 2022), pp. 31120–31125. ISSN: 24701343. DOI: 10.1021/AC SOMEWA.2C03257 / ASSET / IMAGES / LARGE / AO2C03257_0004.JPEG. URL: <https://pubs.acs.org/doi/full/10.1021/acsomega.2c03257>.
- [28] Kenzo Maehashi, Taiji Katsura, Kagan Kerman, et al. “Label-free protein biosensor based on aptamer-modified carbon nanotube field-effect transistors”. In: *Analytical Chemistry* 79.2 (Jan. 2007), pp. 782–787. ISSN: 00032700. DOI: 10.1021/ac060830g. URL: <https://pubs.acs.org/doi/full/10.1021/ac060830g>.
- [29] Cristina García-Aljaro, Lakshmi N. Cella, Dhamanand J. Shirale, et al. “Carbon nanotubes-based chemiresistive biosensors for detection of microorganisms”. In: *Biosensors and Bioelectronics* 26.4 (Dec. 2010), pp. 1437–1441. ISSN: 09565663. DOI: 10.1016/j.bios.2010.07.077.
- [30] R. J. Chen, Y. Zhang, D. Wang, et al. “Noncovalent sidewall functionalization of single-walled carbon nanotubes for protein immobilization”. In: *Journal of the American Chemical Society* 123.16 (2001), pp. 3838–3839. ISSN: 00027863. DOI: 10.1021/ja010172b. URL: <http://pubs.acs.org..>
- [31] Lakshmi N. Cella, Pablo Sanchez, Wenwan Zhong, et al. “Nano aptasensor for Protective Antigen Toxin of Anthrax”. In: *Analytical Chemistry* 82.5 (Mar. 2010), pp. 2042–2047. ISSN: 00032700. DOI: 10.1021/ac902791q. URL: <https://pubs.acs.org/doi/full/10.1021/ac902791q>.

- [32] Basanta K. Das, Chaker Tlili, Sushmee Badhulika, et al. “Single-walled carbon nanotubes chemiresistor aptasensors for small molecules: Picomolar level detection of adenosine triphosphate”. In: *Chemical Communications* 47.13 (Mar. 2011), pp. 3793–3795. ISSN: 1364548X. DOI: 10.1039/c0cc04733c. URL: <https://pubs.rsc.org/en/content/articlehtml/2011/cc/c0cc04733c%20https://pubs.rsc.org/en/content/articlelanding/2011/cc/c0cc04733c>.
- [33] Koen Besteman, Jeong O. Lee, Frank G.M. Wiertz, et al. “Enzyme-coated carbon nanotubes as single-molecule biosensors”. In: *Nano Letters* 3.6 (June 2003), pp. 727–730. ISSN: 15306984. DOI: 10.1021/NL034139U. URL: <https://pubs.acs.org/doi/full/10.1021/nl034139u>.
- [34] Deana Kwong Hong Tsang, Tyler J. Lieberthal, Clare Watts, et al. “Chemically Functionalised Graphene FET Biosensor for the Label-free Sensing of Exosomes”. In: *Scientific Reports* 9.1 (Sept. 2019), pp. 1–10. ISSN: 20452322. DOI: 10.1038/s41598-019-50412-9. URL: <https://www.nature.com/articles/s41598-019-50412-9>.
- [35] Gregory R. Wiedman, Yanan Zhao, Arkady Mustaev, et al. “An Aptamer-Based Biosensor for the Azole Class of Antifungal Drugs”. In: *mSphere* 2.4 (Aug. 2017). ISSN: 23795042. DOI: 10.1128/msphere.00274-17. URL: [/pmc/articles/PMC5566834/](https://pmc/articles/PMC5566834/) %20 / pmc / articles / PMC5566834 / ?report = abstract % 20https://www.ncbi.nlm.nih.gov/pmc/articles/PMC5566834/.
- [36] Zhaoli Gao, Han Xia, Jonathan Zauberman, et al. “Detection of Sub-fM DNA with Target Recycling and Self-Assembly Amplification on Graphene Field-Effect Biosensors”. In: *Nano Letters* 18.6 (June 2018), pp. 3509–3515. ISSN: 15306992. DOI: 10.1021/acs.nanolett.8b00572. URL: <https://pubs.acs.org/doi/full/10.1021/acs.nanolett.8b00572>.
- [37] Michael T. Hwang, B. Landon Preston, Lee Joon, et al. “Highly specific SNP detection using 2D graphene electronics and DNA strand displacement”. In: *Proceedings of the National Academy of Sciences of the United States of America* 113.26 (June 2016), pp. 7088–7093. ISSN: 10916490. DOI: 10.1073/pnas.1603753113. URL: <https://www.pnas.org/doi/abs/10.1073/pnas.1603753113>.
- [38] Zhuang Hao, Yunlu Pan, Cong Huang, et al. “Modulating the Linker Immobilization Density on Aptameric Graphene Field Effect Transistors Using an Electric Field”. In: *ACS Sensors* 5.8 (Aug. 2020), pp. 2503–2513. ISSN: 23793694. DOI: 10.1021/ACSENSORS.0C00752/ASSET/IMAGES/LARGE/SE0C00752_0008.JPEG. URL: <https://pubs.acs.org/doi/full/10.1021/acssensors.0c00752>.
- [39] Mohd Maidin Nur Nasyifa, A. Rahim Ruslinda, Nur Hamidah Abdul Halim, et al. “Immuno-probed graphene nanoplatelets on electrolyte-gated field-effect transistor for stable cortisol quantification in serum”. In: *Journal of the Taiwan Institute of Chemical Engineers* 117 (Dec. 2020), pp. 10–18. ISSN: 18761070. DOI: 10.1016/j.jtice.2020.12.008.

Bibliography

- [40] Rui Campos, Jérôme Borme, Joana Rafaela Guerreiro, et al. “Attomolar label-free detection of dna hybridization with electrolyte-gated graphene field-effect transistors”. In: *ACS Sensors* 4.2 (Feb. 2019), pp. 286–293. ISSN: 23793694. DOI: 10.1021/acssensors.8b00344. URL: <https://pubs.acs.org/doi/full/10.1021/acssensors.8b00344>.
- [41] Murat Kuscu, Hamideh Ramezani, Ergin Dinc, et al. “Graphene-based Nanoscale Molecular Communication Receiver: Fabrication and Microfluidic Analysis”. In: (June 2020). arXiv: 2006.15470. URL: <https://arxiv.org/abs/2006.15470v2>.
- [42] Shicai Xu, Jian Zhan, Baoyuan Man, et al. “Real-time reliable determination of binding kinetics of DNA hybridization using a multi-channel graphene biosensor”. In: *Nature Communications* 8.1 (Mar. 2017), pp. 1–10. ISSN: 20411723. DOI: 10.1038/ncomms14902. URL: <https://www.nature.com/articles/ncomms14902>.
- [43] Niazul I. Khan, Mohammad Mousazadehkasin, Sujoy Ghosh, et al. “An integrated microfluidic platform for selective and real-time detection of thrombin biomarkers using a graphene FET”. In: *Analyst* 145.13 (June 2020), pp. 4494–4503. ISSN: 13645528. DOI: 10.1039/d0an00251h. URL: <https://pubs.rsc.org/en/content/articlehtml/2020/an/d0an00251h%20https://pubs.rsc.org/en/content/articlelanding/2020/an/d0an00251h>.
- [44] T Ono, K Kamada, R Hayashi, et al. “Lab-on-a-graphene-FET detection of key molecular events underpinning influenza 2 virus infection and effect of antiviral drugs 3 Running title: Graphene-FET detects reactions in an influenza infection MAIN TEXT”. In: *bioRxiv* (Mar. 2020), p. 2020.03.18.996884. DOI: 10.1101/2020.03.18.996884. URL: <https://doi.org/10.1101/2020.03.18.996884>.
- [45] Han Yue Zheng, Omar A. Alsager, Bicheng Zhu, et al. “Electrostatic gating in carbon nanotube aptasensors”. In: *Nanoscale* 8.28 (July 2016), pp. 13659–13668. ISSN: 20403372. DOI: 10.1039/c5nr08117c. URL: <https://pubs.rsc.org/en/content/articlehtml/2016/nr/c5nr08117c%20https://pubs.rsc.org/en/content/articlelanding/2016/nr/c5nr08117c>.
- [46] Jun Pyo Kim, Byung Yang Lee, Joohyung Lee, et al. “Enhancement of sensitivity and specificity by surface modification of carbon nanotubes in diagnosis of prostate cancer based on carbon nanotube field effect transistors”. In: *Biosensors and Bioelectronics* 24.11 (July 2009), pp. 3372–3378. ISSN: 09565663. DOI: 10.1016/j.bios.2009.04.048. URL: <https://pubmed.ncbi.nlm.nih.gov/19481922/>.
- [47] Jagriti Sethi, Michiel Van Bulck, Ahmed Suhail, et al. “A label-free biosensor based on graphene and reduced graphene oxide dual-layer for electrochemical determination of beta-amyloid biomarkers”. In: *Microchimica Acta* 187.5 (May 2020), pp. 1–10. ISSN: 14365073. DOI: 10.1007/s00604-020-04267-x. URL: <https://link.springer.com/article/10.1007/s00604-020-04267-x>.

- [48] Yasuhide Ohno, Kenzo Maehashi, and Kazuhiko Matsumoto. “Label-free biosensors based on aptamer-modified graphene field-effect transistors”. In: *Journal of the American Chemical Society* 132.51 (Dec. 2010), pp. 18012–18013. ISSN: 00027863. DOI: 10.1021/ja108127r. URL: <https://pubs.acs.org/doi/full/10.1021/ja108127r>.
- [49] Ryan J. Lopez, Sofia Babanova, Kateryna Artyushkova, et al. “Surface modifications for enhanced enzyme immobilization and improved electron transfer of PQQ-dependent glucose dehydrogenase anodes”. In: *Bioelectrochemistry* 105 (Oct. 2015), pp. 78–87. ISSN: 1878562X. DOI: 10.1016/j.bioelechem.2015.05.010. URL: <https://pubmed.ncbi.nlm.nih.gov/26011132/>.
- [50] Guinevere Strack, Robert Nichols, Plamen Atanassov, et al. “Modification of carbon nanotube electrodes with 1-pyrenebutanoic acid, succinimidyl ester for enhanced bioelectrocatalysis”. In: *Methods in Molecular Biology* 1051 (2013), pp. 217–228. ISSN: 10643745. DOI: 10.1007/978-1-62703-550-7_14. URL: <https://pubmed.ncbi.nlm.nih.gov/23934807/>.
- [51] Greg T. Hermanson. “The Reactions of Bioconjugation”. In: *Bioconjugate Techniques* (Jan. 2013), pp. 229–258. DOI: 10.1016/B978-0-12-382239-0.00003-0.
- [52] Malcolm Hinnemo, Jie Zhao, Patrik Ahlberg, et al. “On Monolayer Formation of Pyrenebutyric Acid on Graphene”. In: *Langmuir* 33.15 (Apr. 2017), pp. 3588–3593. ISSN: 15205827. DOI: 10.1021/ACS.LANGMUIR.6B04237/ASSET/IMAGES/LARGE/LA-2016-04237V_0003.JPG. URL: <https://pubs.acs.org/doi/full/10.1021/acs.langmuir.6b04237>.
- [53] Xue V. Zhen, Emily G. Swanson, Justin T. Nelson, et al. “Noncovalent monolayer modification of graphene using pyrene and cyclodextrin receptors for chemical sensing”. In: *ACS Applied Nano Materials* 1.6 (June 2018), pp. 2718–2726. ISSN: 25740970. DOI: 10.1021/acsanm.8b00420. URL: <https://pubs.acs.org/doi/full/10.1021/acsanm.8b00420>.
- [54] Ryan J. White, Noelle Phares, Arica A. Lubin, et al. “Optimization of electrochemical aptamer-based sensors via optimization of probe packing density and surface chemistry”. In: *Langmuir : the ACS journal of surfaces and colloids* 24.18 (Sept. 2008), pp. 10513–10518. ISSN: 0743-7463. DOI: 10.1021/LA800801V. URL: <https://pubmed.ncbi.nlm.nih.gov/18690727/>.
- [55] Yu Chen, Tze Sian Pui, Patthara Kongsuphol, et al. “Aptamer-based array electrodes for quantitative interferon- γ detection”. In: *Biosensors and Bioelectronics* 53 (Mar. 2014), pp. 257–262. ISSN: 1873-4235. DOI: 10.1016/J.BIOS.2013.09.046. URL: <https://pubmed.ncbi.nlm.nih.gov/24144556/>.
- [56] Greg T. Hermanson. “Homobifunctional Crosslinkers”. In: *Bioconjugate Techniques* (Jan. 2013), pp. 275–298. DOI: 10.1016/B978-0-12-382239-0.00005-4.
- [57] 1-Pyrenebutyric acid N-hydroxysuccinimide ester - [1H NMR] - Spectrum - SpectraBase. URL: <https://spectrabase.com/spectrum/FxRoJanrm9t> (visited on 2023-10-19).

Bibliography

- [58] R. G. Lebel and D. A.I. Goring. “Density, Viscosity, Refractive Index, and Hygroscopicity of Mixtures of Water and Dimethyl Sulfoxide”. In: *Journal of Chemical and Engineering Data* 7.1 (Jan. 1962), pp. 100–101. ISSN: 15205134. DOI: 10.1021/JE60012A032 / ASSET / JE60012A032.FP.PNG_V03. URL: <https://pubs.acs.org/doi/abs/10.1021/je60012a032>.
- [59] Alexander B. Artyukhin, Michael Stadermann, Raymond W. Friddle, et al. “Controlled electrostatic gating of carbon nanotube FET devices”. In: *Nano Letters* 6.9 (Sept. 2006), pp. 2080–2085. ISSN: 15306984. DOI: 10.1021/NL061343J/SUPPL_FILE/NL061343JSI20060609_104449.PDF. URL: <https://pubs.acs.org/doi/full/10.1021/nl061343j>.
- [60] Iddo Heller, Anne M. Janssens, Jaan Männik, et al. “Identifying the mechanism of biosensing with carbon nanotube transistors”. In: *Nano Letters* 8.2 (Feb. 2008), pp. 591–595. ISSN: 15306984. DOI: 10.1021/NL072996I. URL: <https://pubs.acs.org/doi/full/10.1021/nl072996i>.
- [61] M. Mohsen-Nia, H. Amiri, and B. Jazi. “Dielectric constants of water, methanol, ethanol, butanol and acetone: Measurement and computational study”. In: *Journal of Solution Chemistry* 39.5 (2010), pp. 701–708. ISSN: 00959782. DOI: 10.1007/S10953-010-9538-5.
- [62] Johannes Hunger, Richard Buchner, Mohamed E. Kandil, et al. “Relative permittivity of dimethylsulfoxide and N, N -dimethylformamide at temperatures from (278 to 328) K and pressures from (0.1 to 5) MPa”. In: *Journal of Chemical and Engineering Data* 55.5 (May 2010), pp. 2055–2065. ISSN: 00219568. DOI: 10.1021/JE9010773 / SUPPL_FILE / JE9010773_SI_001.PDF. URL: <https://pubs.acs.org/doi/full/10.1021/je9010773>.
- [63] Ning Gao, Teng Gao, Xiao Yang, et al. “Specific detection of biomolecules in physiological solutions using graphene transistor biosensors”. In: *Proceedings of the National Academy of Sciences of the United States of America* 113.51 (Dec. 2016), pp. 14633–14638. ISSN: 10916490. DOI: 10.1073/PNAS.1625010114 / SUPPL_FILE / PNAS.201625010SI.PDF. URL: <https://www.pnas.org/doi/abs/10.1073/pnas.1625010114>.
- [64] Kyoungseon Min, Jungbae Kim, Kyungmoon Park, et al. “Enzyme immobilization on carbon nanomaterials: Loading density investigation and zeta potential analysis”. In: *Journal of Molecular Catalysis B: Enzymatic* 83 (Nov. 2012), pp. 87–93. ISSN: 1381-1177. DOI: 10.1016/J.MOLCATB.2012.07.009.
- [65] Xuan Xu, Jiachao Yu, Jing Qian, et al. “Functionalization of nitrogen-doped carbon nanotubes by 1-pyrenebutyric acid and its application for biosensing”. In: *IEEE Sensors Journal* 14.7 (2014), pp. 2341–2346. ISSN: 1530437X. DOI: 10.1109/JSEN.2014.2309974.

- [66] Mercè Pachos, Iñigo Martin-Fernandez, Xavier Borrisé, et al. “Real time protein recognition in a liquid-gated carbon nanotube field-effect transistor modified with aptamers”. In: *Nanoscale* 4.19 (Sept. 2012), pp. 5917–5923. ISSN: 2040-3372. DOI: 10.1039/C2NR31257C. URL: <https://pubs.rsc.org/en/content/articlehtml/2012/nr/c2nr31257c>.
- [67] Marcin S. Filipiak, Marcel Rother, Nesha M. Andoy, et al. “Highly sensitive, selective and label-free protein detection in physiological solutions using carbon nanotube transistors with nanobody receptors”. In: *Sensors and Actuators B: Chemical* 255 (Feb. 2018), pp. 1507–1516. ISSN: 0925-4005. DOI: 10.1016/J.SNB.2017.08.164.
- [68] Jie Liu, Florence Appaix, Olivier Bibari, et al. “Control of neuronal network organization by chemical surface functionalization of multi-walled carbon nanotube arrays”. In: *Nanotechnology* 22.19 (May 2011). ISSN: 1361-6528. DOI: 10.1088/0957-4484/22/19/195101. URL: <https://pubmed.ncbi.nlm.nih.gov/21436508/>.
- [69] Christoph Fenzl, Pranati Nayak, Thomas Hirsch, et al. “Laser-Scribed Graphene Electrodes for Aptamer-Based Biosensing”. In: *ACS sensors* 2.5 (May 2017), pp. 616–620. ISSN: 2379-3694. DOI: 10.1021/ACSSENSORS.7B00066. URL: <https://pubmed.ncbi.nlm.nih.gov/28723173/>.
- [70] Deepak Sehgal and Inder K. Vijay. “A Method for the High Efficiency of Water-Soluble Carbodiimide-Mediated Amidation”. In: *Analytical Biochemistry* 218.1 (Apr. 1994), pp. 87–91. ISSN: 0003-2697. DOI: 10.1006/ABIO.1994.1144.
- [71] Greg T. Hermanson. “Zero-Length Crosslinkers”. In: *Bioconjugate Techniques* (Jan. 2013), pp. 259–273. DOI: 10.1016/B978-0-12-382239-0.00004-2.
- [72] Greg T. Hermanson. “Microparticles and Nanoparticles”. In: *Bioconjugate Techniques* (Jan. 2013), pp. 549–587. DOI: 10.1016/B978-0-12-382239-0.00014-5.
- [73] Gang Wei, Changjiang Pan, Jörg Reichert, et al. “Controlled assembly of protein-protected gold nanoparticles on noncovalent functionalized carbon nanotubes”. In: *Carbon* 48.3 (Mar. 2010), pp. 645–653. ISSN: 0008-6223. DOI: 10.1016/J.CARBON.2009.10.006.
- [74] Meng Lan, Guoli Fan, Wei Sun, et al. “Synthesis of hybrid Zn–Al–In mixed metal oxides/carbon nanotubes composite and enhanced visible-light-induced photocatalytic performance”. In: *Applied Surface Science* 282 (Oct. 2013), pp. 937–946. ISSN: 0169-4332. DOI: 10.1016/J.APSUSC.2013.06.095.
- [75] Mitchell B. Lerner, James M. Resczenski, Akshay Amin, et al. “Toward quantifying the electrostatic transduction mechanism in carbon nanotube molecular sensors”. In: *Journal of the American Chemical Society* 134.35 (Sept. 2012), pp. 14318–14321. ISSN: 00027863. DOI: 10.1021/JA306363V/SUPPL_FILE/JA306363V_SI_001.PDF. URL: <https://pubs.acs.org/doi/full/10.1021/ja306363v>.

Bibliography

- [76] Michael Holzinger, Jessica Baur, Raoudha Haddad, et al. “Multiple functionalization of single-walled carbon nanotubes by dip coating”. In: *Chemical Communications* 47.8 (Feb. 2011), pp. 2450–2452. ISSN: 1364-548X. DOI: 10.1039/C0CC03928D. URL: <https://pubs.rsc.org/en/content/articlehtml/2011/cc/c0cc03928d> % 20<https://pubs.rsc.org/en/content/articlelanding/2011/cc/c0cc03928d>.
- [77] Yoshihisa Amano, Ayako Koto, Shohei Matsuzaki, et al. “Construction of a biointerface on a carbon nanotube surface for efficient electron transfer”. In: *Materials Letters* 174 (July 2016), pp. 184–187. ISSN: 0167-577X. DOI: 10.1016/J.MATLET.2016.03.113.
- [78] Y. Y. Chang, H. Li, and H. Sun. “Immobilized Metal Affinity Chromatography (IMAC) for Metalloproteomics and Phosphoproteomics”. In: *Inorganic and Organometallic Transition Metal Complexes with Biological Molecules and Living Cells* (Jan. 2017), pp. 329–353. DOI: 10.1016/B978-0-12-803814-7.00009-5.
- [79] Alexander Star, Jean Christophe P. Gabriel, Keith Bradley, et al. “Electronic detection of specific protein binding using nanotube FET devices”. In: *Nano Letters* 3.4 (Apr. 2003), pp. 459–463. ISSN: 15306984. DOI: 10.1021/NL0340172. URL: <https://pubs.acs.org/doi/full/10.1021/nl0340172>.
- [80] Christopher M. Dundas, Daniel Demonte, and Sheldon Park. “Streptavidin-biotin technology: Improvements and innovations in chemical and biological applications”. In: *Applied Microbiology and Biotechnology* 97.21 (Nov. 2013), pp. 9343–9353. ISSN: 01757598. DOI: 10.1007/S00253-013-5232-Z/FIGURES/3. URL: <https://link.springer.com/article/10.1007/s00253-013-5232-z>.
- [81] Greg T. Hermanson. “(Strept)avidin–Biotin Systems”. In: *Bioconjugate Techniques* (Jan. 2013), pp. 465–505. DOI: 10.1016/B978-0-12-382239-0.00011-X.
- [82] Michael Fairhead and Mark Howarth. “Site-specific biotinylation of purified proteins using BirA”. In: *Methods in molecular biology (Clifton, N.J.)* 1266 (2015), p. 171. ISSN: 10643745. DOI: 10.1007/978-1-4939-2272-7_12. URL: /pmc/articles/PMC4304673/ %20/pmc/articles/PMC4304673/ ?report=abstract % 20<https://www.ncbi.nlm.nih.gov/pmc/articles/PMC4304673/>.
- [83] Greg T. Hermanson. “PEGylation and Synthetic Polymer Modification”. In: *Bioconjugate Techniques* (Jan. 2013), pp. 787–838. DOI: 10.1016/B978-0-12-382239-0.00018-2.
- [84] Mehdi Meran, Pelin Deniz Akkus, Ozge Kurkcuoglu, et al. “Noncovalent Pyrene-Polyethylene Glycol Coatings of Carbon Nanotubes Achieve in Vitro Biocompatibility”. In: *Langmuir* 34.40 (Oct. 2018), pp. 12071–12082. ISSN: 15205827. DOI: 10.1021/ACS.LANGMUIR.8B00971. URL: <https://pubs.acs.org/doi/full/10.1021/acs.langmuir.8b00971>.

- [85] Hiroko Miki, Atsunobu Isobayashi, Tatsuro Saito, et al. “Ionic liquids with wafer-scalable graphene sensors for biological detection”. In: *IEEE Transactions on Nanobioscience* 18.2 (Apr. 2019), pp. 216–219. ISSN: 15361241. DOI: 10.1109/TNB.2019.2905286.
- [86] Nozomi Nakayama-Ratchford, Sarunya Bangsaruntip, Xiaoming Sun, et al. “Non-Covalent Functionalization of Carbon Nanotubes by Fluorescein-Polyethylene Glycol: Supramolecular Conjugates with pH Dependent Absorbance and Fluorescence”. In: *Journal of the American Chemical Society* 129.9 (Mar. 2007), p. 2448. ISSN: 00027863. DOI: 10.1021/JA068684J. URL: /pmc/articles/PMC4161124/%20/pmc/articles/PMC4161124/?report=abstract%20https://www.ncbi.nlm.nih.gov/pmc/articles/PMC4161124/.
- [87] Zhenghai Tang, Yanda Lei, Baochun Guo, et al. “The use of rhodamine B-decorated graphene as a reinforcement in polyvinyl alcohol composites”. In: *Polymer* 53.2 (Jan. 2012), pp. 673–680. ISSN: 0032-3861. DOI: 10.1016/J.POLYMER.2011.11.056.
- [88] Maria G. Khrenova, Alexander V. Nemukhin, and Vladimir G. Tsirelson. “Origin of the π -stacking induced shifts in absorption spectral bands of the green fluorescent protein chromophore”. In: *Chemical Physics* 522 (June 2019), pp. 32–38. ISSN: 0301-0104. DOI: 10.1016/J.CHEMPHYS.2019.02.010.
- [89] Yuan Qiu, Haisi Hu, Dongxu Zhao, et al. “Concentration-dependent dye aggregation and disassembly triggered by the same artificial helical foldamer”. In: *Polymer* 170 (Apr. 2019), pp. 7–15. ISSN: 0032-3861. DOI: 10.1016/J.POLYMER.2019.02.063.
- [90] Jeng Hao Pai, Yuli Wang, Gina To A. Salazar, et al. “A Photoresist with Low Fluorescence for Bioanalytical Applications”. In: *Analytical chemistry* 79.22 (Nov. 2007), p. 8774. ISSN: 00032700. DOI: 10.1021/AC071528Q. URL: /pmc/articles/PMC2435225/%20/pmc/articles/PMC2435225/?report=abstract%20https://www.ncbi.nlm.nih.gov/pmc/articles/PMC2435225/.
- [91] Ali Ashraf, Yanbin Wu, Michael C. Wang, et al. “Spectroscopic investigation of the wettability of multilayer graphene using highly ordered pyrolytic graphite as a model material”. In: *Langmuir* 30.43 (Nov. 2014), pp. 12827–12836. ISSN: 15205827. DOI: 10.1021/LA503089K/SUPPL_FILE/LA503089K_SI_001.PDF. URL: https://pubs.acs.org/doi/full/10.1021/la503089k.
- [92] András Pálkás, György Kálvin, Péter Vancsó, et al. “The composition and structure of the ubiquitous hydrocarbon contamination on van der Waals materials”. In: *Nature Communications* 2022 13:1 13.1 (Nov. 2022), pp. 1–10. ISSN: 2041-1723. DOI: 10.1038/s41467-022-34641-7. arXiv: 2207.01057. URL: https://www.nature.com/articles/s41467-022-34641-7.
- [93] Grzegorz Stando, Damian Łukawski, Filip Lisiecki, et al. “Intrinsic hydrophilic character of carbon nanotube networks”. In: *Applied Surface Science* 463 (Jan. 2019), pp. 227–233. ISSN: 0169-4332. DOI: 10.1016/J.APSUSC.2018.08.206.

Bibliography

- [94] Minsuk Park, In Seung Choi, and Sang Yong Ju. “Quantification and removal of carbonaceous impurities in a surfactant-assisted carbon nanotube dispersion and its implication on electronic properties”. In: *Nanoscale Advances* 4.17 (Aug. 2022), pp. 3537–3548. ISSN: 2516-0230. DOI: 10.1039/D2NA00153E. URL: <https://pubs.rsc.org/en/content/articlehtml/2022/na/d2na00153e%20https://pubs.rsc.org/en/content/articlelanding/2022/na/d2na00153e>.
- [95] Young Jun Shin, Yingying Wang, Han Huang, et al. “Surface-energy engineering of graphene”. In: *Langmuir* 26.6 (Mar. 2010), pp. 3798–3802. ISSN: 07437463. DOI: 10.1021/LA100231U/ASSET/IMAGES/LARGE/LA-2010-00231U_0005.JPG. URL: <https://pubs.acs.org/doi/full/10.1021/la100231u>.
- [96] Creative PEGWorks. *Functionalisation with Pyrene-PEG-Rhodamine*. 2022.
- [97] Robert D. Deegan, Olgica Bakajin, Todd F. Dupont, et al. “Capillary flow as the cause of ring stains from dried liquid drops”. In: *Nature* 1997 389:6653 389.6653 (1997), pp. 827–829. ISSN: 1476-4687. DOI: 10.1038/39827. URL: <https://www.nature.com/articles/39827>.
- [98] Shunsuke F. Shimabayashi, Mikiko Tsudome, and Tomo Kurimura. “Suppression of the coffee-ring effect by sugar-assisted depinning of contact line”. In: *Scientific Reports* 2018 8:1 8.1 (Dec. 2018), pp. 1–9. ISSN: 2045-2322. DOI: 10.1038/s41598-018-35998-w. URL: <https://www.nature.com/articles/s41598-018-35998-w>.